Progress In Electromagnetics Research B, Vol. 16, 21–56, 2009

THE RELATIVISTIC HERMITE POLYNOMIALS AND THE WAVE EQUATION

A. Torre

ENEA-FIM-FISMAT Tecnologie Fisiche e Nuovi Materiali
via E. Fermi 45, Frascati, Rome 00044, Italy

Abstract—Solutions of the homogeneous 2D scalar wave equation of a type reminiscent of the "splash pulse" waveform are investigated in some detail. In particular, it is shown that the "higher-order" solutions relative to a given "fundamental" one, from which they are obtained through a definite "generation scheme", come to involve the relativistic Hermite polynomials. This parallels the results of a previous work, where solutions of the 3D wave equation involving the relativistic Laguerre polynomials have been suggested. Then, exploiting a well known rule, the obtained wave functions are used to construct further solutions of the 3D wave equation. The link of the resulting wave functions with those analyzed in the previous work is clarified, the pertinent generation scheme being indeed inferred. Finally, solutions of the Klein-Gordon equation which relate to such Lorentzian-like solutions of the scalar wave equation are deduced.

1. INTRODUCTION

The literature concerned with the homogeneous 3D scalar wave equation,

$$\left[\nabla^2 - c^{-2}\partial_t^2\right] u\left(x, y, z, t\right) = 0, \tag{1}$$

is rich of transformations which allow us to pass from one solution (or, *wave function*) to another [1–7]. Needless to say, here $u\left(x, y, z, t\right)$ represents the scalar-valued wave field and c is the (constant) speed of propagation; also, (x, y, z) denote Cartesian coordinates, with in particular z being assumed along the direction of propagation, and, of course, $\nabla^2 = \partial_x^2 + \partial_y^2 + \partial_z^2$.

In this connection, further hints have been recently suggested in [8] and [9], on the basis of the method of incomplete separation of variables

Corresponding author: A. Torre (amalia.torre@enea.it).

and the application of the Bateman conformal transformation. Such approaches have then been framed in [10] within the context of the bidirectional spectral representation [11], which is shown to allow, when examined in conjuction with Bateman's transformations, a systematic derivation of extended families of focus wave mode-type localized solutions of (1).

In particular, as is well known, one can pass from solutions of the 2D wave equation

$$\left[\partial_q^2 + \partial_z^2 - c^{-2}\partial_t^2\right]\phi\,(q,z,t) = 0, \tag{2}$$

where q denotes any one of the two Cartesian coordinate x, y, to solutions of the 3D wave Equation (1) according to the rule [1–7, 12]

$$u(x,y,z,t) = (x \pm iy)^{-\frac{1}{2}}\phi(r,z,t), \quad r = \sqrt{x^2+y^2}. \tag{3}$$

In addition, due to the symmetry of both (1) and (2), it is possible to generate further solutions from a known one by circular permutations of both the space and the time coordinates, i.e., through $q \leftrightarrow z \leftrightarrow \pm ict$ for (2) and $x \leftrightarrow y \leftrightarrow z \leftrightarrow \pm ict$ for (1). Accordingly, (3) is paralleled by another non trivial rule, obtained by transforming the time coordinate into a space coordinate to yield

$$u(x,y,z,t) = (x \pm ct)^{-\frac{1}{2}}\phi\left(\sqrt{x^2-c^2t^2}, z, -\frac{i}{c}y\right). \tag{4}$$

Here, we are concerned with the transformation (3), which will be applied to what can be regarded as the 2D versions of the *splash pulses* [13–16], that is, to 2D wave functions of the type

$$\phi(q,z,t) = \frac{1}{\sqrt{\tau - iz_0}}\left(\sigma + ia + \frac{q^2}{\tau - iz_0}\right)^{-N} \tag{5}$$

where τ and σ signify the characteristic variables $\tau = z - ct$ and $\sigma = z + ct$, N is here taken as a real positive parameter, and similarly z_0 and a are positive parameters with dimensions of length.

A renewed interest in the splash pulses

$$s_\delta(x,y,z,t) = \frac{1}{\tau - iz_0}\frac{1}{\left(\sigma + ia + \frac{r^2}{\tau - iz_0}\right)^\delta}, \tag{6}$$

have been stimulated by the recent analysis presented in [16], where the authors investigated the behavior of the so-called double-exponential (DEX) pulses, obtained as a suitable superposition of progressive

and regressive splash pulses (6), corresponding to in general different values of the parameter a. Specifically, a detailed analysis of the behavior of the splash and DEX pulses for values of δ within the range $-0.9 \leq \delta \leq 0.9$ is presented in the quoted reference.

Also, in [17] and [18] the expression for $s_1(x, y, z, t) = \frac{1}{(\sigma+ia)(\tau-iz_0)+r^2}$ has been taken as a Hertz potential, respectively oriented parallel and orthogonal to the z-direction, from which the components of the corresponding vector electromagnetic fields have then been derived. An extensive study of the field solutions, resulting respectively in toroidal, focused doughnut wave packets and oblate wave packets, have been performed in the quoted references specifically in the *paraxial* regime $z_0 \ll a$. In particular, in [18] the paraxial solutions there analyzed have been demonstrated to be the natural spatiotemporal modes of an open electromagnetic cavity and accordingly their physical realization has been suggested by excitation of a curved mirror resonator or by propagation along the equivalent lens waveguide.

The splash pulses for $\delta > \frac{1}{2}$ have been reconsidered in [19], where the relevant higher-order pulses (there referred to as Laguerre-Lorentzian solutions of (1)), obtained through a definite generation scheme demanding for integer powers of the transverse Laplacian $\nabla_\perp^2 = \partial_x^2 + \partial_y^2$ acting on the Lorentz-like complex function (6)[†], have been related to the relativistic Laguerre polynomials (RLP). In the same reference, the expressions of the electromagnetic field components, corresponding to the Laguerre-Lorentzian wave functions, have been derived in particular for the TE modes, and so for a z-directed Hertz vector potential.

Paralleling the analysis developed in [19], we will show here that higher-order solutions of the 2D wave Equation (2), obtained from the fundamental one (5) acting on it by powers of the derivative operator ∂_q, relate to the relativistic Hermite polynomials (RHP), which so come to modulate the Lorentzian-like factor in the same way as the ordinary Hermite polynomials (HP) modulate the Gaussian-like factor in the 2D Hermite-Gaussian pulses [20–24]. Indeed, in the solutions discussed in [19], the RLPs enter as modulating factors of suitable Lorentz-like functions in the same way as the ordinary Laguerre polynomials (LP) modulate appropriate Gaussian-like functions in the Laguerre-Gaussian pulses [20–24].

[†] Although it is quite an improper terminology, by Lorentz-like (in general, complex) functions we mean here functions of the type $(1 + \frac{\xi^2}{A})^{-B}$, where ξ denotes the coordinate of concern, A is a complex constant (i.e., independent on ξ) and $B > 0$. Clearly, when referred to a wave function, as in the present context, it will not in general yield a similar Lorentz-like behavior (with respect to ξ) for the corresponding wave amplitude.

Then, applying the transformation (3), we will pass from the obtained solutions of the 2D wave equation to wave functions for the 3D wave equation, which so will have the RHPs as their central part. Interestingly we will be successful on deducing among others, a generation scheme for the resulting 3D wave functions, that resorts to the same fundamental form of the solutions considered in [19], but demands for half-integer powers of the same operators involved in the generation scheme pertaining to those solutions. This unequivocally establishes a link of the wave functions discussed here with those suggested in [19]. It is from this link that, in our opinion, the analysis developed here stems its interest, as it allows us to encompass all the wave functions of the splash pulse-type (for positive exponents) discussed here and in the previous paper [19] in a single scheme, which basically resorts to the same symmetry operators of the 3D wave equation. It is in fact evident that what we have referred to as "generation scheme" arises from definite symmetries of the wave equation [5], and hence might comprise and possibly extend already known transformations.

We will not dwell here on the practical feasibility of the solutions of concern in the present context, addressing the issue to future work. We note in fact through Bateman's words ([4], P. 25) that *the theory of wave-functions forms a natural extension of the theory of functions of complex variable and may consequently lead to results of great value for the general theory of functions.* Of course, the possibility of application to physical problems would surely increase the interest in the analysis here presented and would motivate further investigations.

Finally, possible solutions of the Klein-Gordon equation, which strictly relate to the Lorentzian-like wave functions, will be deduced and properly commented on in relation with pertinent results, already existing in the literature.

Let us recall now that the RHPs have been introduced less than two decades ago within the context of the dynamics of the quantum relativistic 1D harmonic oscillator [25]; also, they have recently been re-considered within the context of the paraxial wave propagation in [26], where their relation with the Lorentz beams has been evidenced. Likewise, the RLPs stand out as the relativistic version of the ordinary LPs, their relation to the latter paralleling that of the RHPs to the ordinary HPs as far as the "relativistic" parameter N is concerned [27].

Notably, both the RHPs and the RLPs are not independent polynomials, being indeed proved to relate to the Jacobi polynomials of suitable parameters and arguments [27–29]; specifically, the RHPs relate to the Gegenbauer polynomials. However, since their formal expressions allow for a direct analogy with the Hermite-Gaussian and

Laguerre-Gaussian solutions to the wave equations, we prefer to use such formal expressions and to refer to them in accord with the original terminology, which has also the advantage of evoking the "relativistic" context where those expressions naturally frame.

It is worth noting that the presence of the RHPs, which as recalled relate to the Gegenbauer polynomials, arising in connection with the 2D wave equation is in a sense not surprising indeed, since the symmetry properties of such an equation naturally relate it to the Gegenbauer polynomials [5].

The plan of the paper is as follows. In Section 2, the basic properties of the RHPs are listed. In Section 3, we relate the RHPs to the solutions of the 2D wave Equation (2). Consequences of the transformation (3) are then investigated in Section 4, where generation schemes for the introduced *Hermite-Lorentzian* solutions of the 3D wave Equation (1) are deduced; in particular, we clarify in Section 5 the link of the obtained wave functions with the Laguerre-Lorentzian solutions, considered in [19]. Solutions of the Klein-Gordon equation, which relate to those of the scalar wave equation discussed in the previous sections, are finally deduced in Section 6. Concluding notes are given in Section 7.

2. THE RELATIVISTIC HERMITE POLYNOMIALS: BASIC PROPERTIES

The RHPs $H_n^{(N)}(\xi)$ have been originally introduced in the form [25]

$$H_n^{(N)}(\xi) = \frac{n!}{2^n} \frac{\Gamma\left(N+\frac{1}{2}\right)}{N^{\frac{n}{2}}} \frac{\Gamma(2N+n)}{\Gamma(2N)} \sum_{j=0}^{\left[\frac{n}{2}\right]} \frac{(-)^j}{j!(n-2j)!} \frac{1}{\Gamma\left(N+j+\frac{1}{2}\right)} \left(\frac{2\xi}{\sqrt{N}}\right)^{n-2j}, \quad -\infty<\xi<+\infty \tag{7}$$

for positive real value of the dimensionless parameter N, as the polynomial component of the quantum relativistic harmonic oscillator wave function. The parameter N, defined by the ratio of the oscillator energy mc^2 to the its quantum of energy $\hbar\omega_0$: $N = \frac{mc^2}{\hbar\omega_0}$, signals the "relativistic" character of the polynomials (7), which in fact in the asymptotic (non-relativistic) limit, $c \to \infty$ (i.e., $N \to \infty$) turn into the ordinary Hermite polynomials $H_n(\xi)$ (HP).

As mentioned earlier, the RHPs relate to the GPs C_n^N, being

indeed

$$H_n^{(N)}(\xi) = \frac{n!}{N^{\frac{n}{2}}} \left(1 + \frac{\xi^2}{N}\right)^{\frac{n}{2}} C_n^N \left(\frac{\xi}{\sqrt{N}\left(1 + \frac{\xi^2}{N}\right)^{\frac{1}{2}}}\right). \tag{8}$$

The polynomials (7) are even or odd according to the evenness of the index n, since $H_n^{(N)}(-\xi) = (-)^n H_n^{(N)}(\xi)$. Furthermore, $H_0^{(N)}(\xi) = 1$ and

$$H_n^{(N)}(0) = \begin{cases} 0, & n = 2m+1 \\ (-)^m \frac{2^n}{N^m} \left(\frac{1}{2}\right)_m (N)_m, & n = 2m\ . \end{cases}$$

Also, as a basic characterization of the RHPs we write down

(i) the differentiation formula

$$\frac{d}{d\xi} H_n^{(N)}(\xi) = \frac{n}{N}(2N + n - 1) H_{n-1}^{(N)}(\xi), \tag{9}$$

(ii) the recurrence relation

$$H_{n+1}^{(N)}(\xi) = 2\left(1 + \frac{n}{N}\right)\xi H_n^{(N)}(\xi) - \left(1 + \frac{\xi^2}{N}\right)\frac{d}{d\xi} H_n^{(N)}(\xi), \tag{10}$$

(iii) the differential equation

$$\left\{\left(1+\frac{\xi^2}{N}\right)\frac{d^2}{d\xi^2} - 2\left(1+\frac{n-1}{N}\right)\xi\frac{d}{d\xi} + 2n\left(1+\frac{n-1}{2N}\right)\right\} H_n^{(N)}(\xi) = 0, \tag{11}$$

(iv) the orthogonality relation

$$\begin{aligned} &\int_{-\infty}^{\infty} \left(1 + \frac{\xi^2}{N}\right)^{-\left(N + \frac{n+m}{2} + 1\right)} H_n^{(N)}(\xi) H_m^{(N)}(\xi) d\xi \\ &= \pi n! \frac{2^{1-2N}}{N^{n-\frac{1}{2}}} \frac{\Gamma(2N+n)}{(N+n)\Gamma(N)^2} \delta_{n,m}, \end{aligned} \tag{12}$$

(v) the Rodrigues representation

$$H_n^{(N)}(\xi) = (-)^n \left(1 + \frac{\xi^2}{N}\right)^{N+n} \frac{d^n}{d\xi^n} \left(1 + \frac{\xi^2}{N}\right)^{-N}. \tag{13}$$

Then, we resort to the *Hermite-Lorentzian* functions (HLF) introduced in [26] as

$$\Phi_n^{(N)}(\xi) = H_n^{(N)}(\xi)\left(1+\frac{\xi^2}{N}\right)^{-(N+n)}, \tag{14}$$

which, as there noted, due to the limit relation $(1+\frac{\xi^2}{N})^{-N} \xrightarrow[N\to\infty]{} e^{-\xi^2}$, can be considered as the "relativistic" limit of the elegant Hermite-Gaussian functions (EHGF) $\Phi_n^{(\infty)}(\xi) = H_n(\xi)e^{-\xi^2}$.

It is worth noting that in [26] the parameter N has been limited to integer values only, in order to properly refer to the factor $(1+\frac{\xi^2}{N})^{-(N+n)}$ entering (14) as a Lorentzian $(N+n=1)$ or a multi-Lorentzian $(N+n>1)$ function as well as to work out explicit analytical representations of the propagated beams. Here, we relax such a constraint on N, letting it be an arbitrary positive real number, whilst retaining in a rather improper use, as already noted in the footnote on P. 3, the terminology of Lorentz-like function when referring to the aforementioned factor.

Figure 1 shows the plots of the HLFs for some values of n and N. To help insight into the behavior of such functions the corresponding EHGFs for each n value — the correspondence being intended in the sense of the above mentioned limit relation — are also plotted in the figure. Actually, the graphs reproduce the normalized functions [26]

$$\varphi_n^{(N)}(\xi) = \mathcal{N}_n^{(N)} H_n^{(N)}(\xi)\left(1+\frac{\xi^2}{N}\right)^{-(N+n)}, \tag{15}$$

with $\mathcal{N}_n^{(N)} = 2^N\Gamma(N)[\frac{N^{n-\frac{1}{2}}\Gamma(N+n+\frac{1}{2})}{2\sqrt{\pi}\Gamma(N+n)\Gamma(2N+n-\frac{1}{2})\Gamma(n+\frac{1}{2})}]^{\frac{1}{2}}$, the corresponding normalized EHGFs being $\varphi_n^{(\infty)}(\xi) = \frac{1}{\sqrt{2^{n-\frac{1}{2}}\Gamma(n+\frac{1}{2})}} H_n(\xi)e^{-\xi^2}$.

As to the normalization factor $\mathcal{N}_n^{(N)}$ entering (15), we see that it can easily be evaluated by resorting to the Parseval theorem and to the possibility of representing the $\Phi_n^{(N)}$'s as [26]

$$\Phi_n^{(N)}(\xi) = \widehat{\mathcal{F}}^{-1}(-i\kappa)^n\widehat{\mathcal{F}}\left(1+\frac{\xi^2}{N}\right)^{-N}$$

as a consequence of the Rodrigues Formula (13); here, $\widehat{\mathcal{F}}$ signifies Fourier transform. We note that

$$\widehat{\mathcal{F}}\left(1+\frac{\xi^2}{N}\right)^{-N} = \frac{\sqrt{\pi}}{2^{N-\frac{3}{2}}}\frac{N^{N-\frac{1}{2}}}{\Gamma(N)}|\kappa|^{N-1}W_{0,\,N-\frac{1}{2}}\left(2\sqrt{N}|\kappa|\right), \tag{16}$$

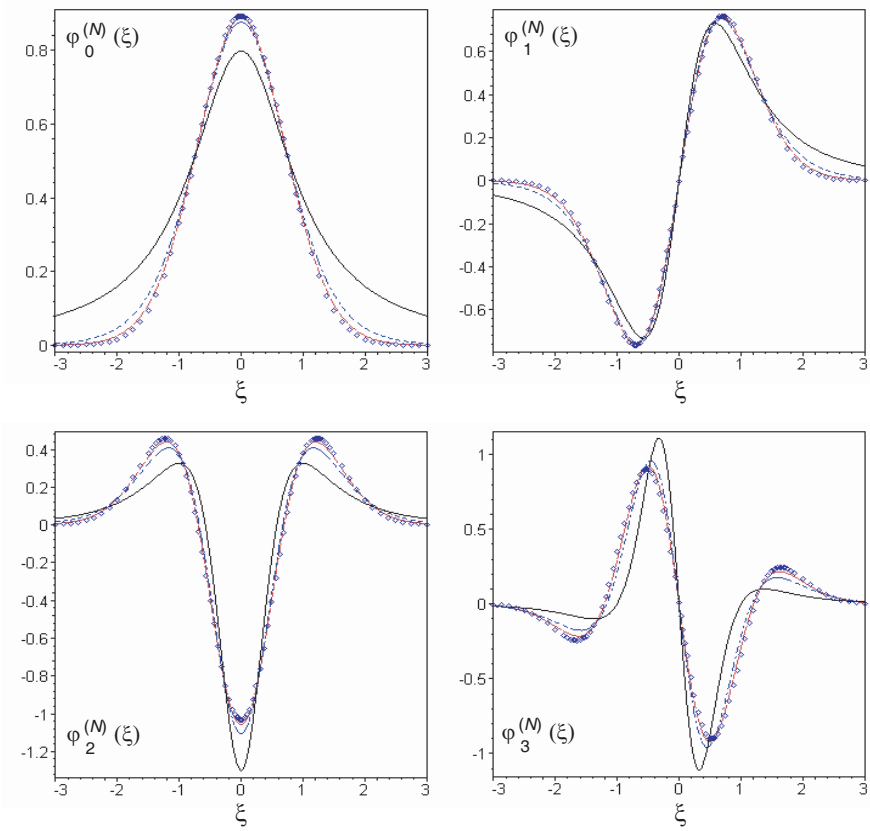

Figure 1. ξ-profiles of the HLFs $\varphi_n^{(N)}$'s for $n = 0, 1, 2, 3$ and $N = 1$ (solid line), $N = 5$ (dash-dotted line), $N = 15$ (dashed line). The profiles of the corresponding EHGFs $\varphi_n^{(\infty)}$ for each value of n are also plotted, marked by the $\diamondsuit$'s.

where $W_{\nu,\mu}$ denotes Whittaker's second function [30].

Accordingly, the integral representation of $\Phi_n^{(N)}(\xi)$ follows in the form

$$\Phi_n^{(N)}(\xi) = \frac{(-i)^n}{2^{N-2}} \frac{N^{N-\frac{1}{2}}}{\Gamma(N)} \int_0^\infty \begin{Bmatrix} \cos(\kappa\xi) & n \text{ even} \\ i\sin(\kappa\xi) & n \text{ odd} \end{Bmatrix} \kappa^{N+n-1} W_{0,N-\frac{1}{2}}\left(2\sqrt{N}\kappa\right) d\kappa. \quad (17)$$

In this connection, we recall that $W_{0,\mu}(z) = \sqrt{\frac{z}{\pi}} K_\mu(\frac{z}{2})$, K_μ being the modified Bessel function of second kind; such a relation may help the comparison of (17) with the expression of the integral representation of

the Laguerre-Lorentzian functions discussed in [19] (see Equation (29) there).

Also, the differential equation for the $\Phi_n^{(N)}$'s is easily obtained as

$$\left\{\left(1+\frac{\xi^2}{N}\right)\frac{d^2}{d\xi^2}+(n+1)\left(\frac{2N+n}{N}\right)\xi\frac{d}{d\xi}+2\left(\frac{N+n+1}{N}\right)\right\}\Phi_n^{(N)}(\xi)=0. \quad (18)$$

Finally, for future use we report the relation between the RHPs and the RLPs, i.e.,

$$\begin{aligned} H_{2m}^{(N)}(\xi) &= (-)^m m!2^{2m}\frac{(N)_m}{N^m}L_m^{\left(-\frac{1}{2},N\right)}(\xi^2), \\ H_{2m+1}^{(N)}(\xi) &= (-)^m m!2^{2m+1}\frac{(N)_{m+1}}{N^{m+1}}\xi L_m^{\left(\frac{1}{2},N\right)}(\xi^2), \end{aligned} \quad (19)$$

which is evidently reminiscent of that holding between the ordinary polynomials, recovered indeed in the limit $N \to \infty$ [27]. The RLPs $L_n^{(\alpha,N)}(x)$ are defined by [27]

$$L_n^{(\alpha,\,N)}(x)=\Gamma\left(N+n+\frac{1}{2}\right)\sum_{j=0}^{n}(-)^j\binom{n+\alpha}{n-j}\frac{1}{j!\Gamma\left(N+n-j+\frac{1}{2}\right)}\left(\frac{x}{N}\right)^j, \quad (20)$$

which in the limit $N \to \infty$ turns into the expression for the ordinary Laguerre polynomials $L_n^{(\alpha)}(x)$ [30]. We see that $L_n^{(\alpha,\,N)}(0) = 1$ and $L_0^{(\alpha,\,N)}(x) = 1$; furthermore, the RLPs relate to the Jacobi polynomials $P_n^{(\beta,\alpha)}$, being indeed [27, 29]

$$L_n^{(\alpha,\,N)}(x) = (-)^n\left(1+\frac{x}{N}\right)^n P_n^{\left(N-\frac{1}{2},\alpha\right)}\left(\frac{x-N}{x+N}\right). \quad (21)$$

Also, in order to facilitate subsequent checks we note that

$$L_n^{(-k,\,N)}(x) = (-)^k\frac{(n-k)!}{n!}\left(\frac{x}{N}\right)^k\frac{\Gamma\left(N+n+\frac{1}{2}\right)}{\Gamma\left(N+n-k+\frac{1}{2}\right)}L_{n-k}^{(k,\,N)}(x), \quad (22)$$

with k integer such that $0 \le k \le n$.

3. THE RELATIVISTIC HERMITE POLYNOMIALS AND THE 2D WAVE EQUATION

It is easy to verify that Equation (2) is solved by the function

$$\phi_{0,\,N}(x,z,t) = \frac{1}{\sqrt{\tau - iz_0}}\left(\sigma + ia + \frac{x^2}{\tau - iz_0}\right)^{-N} \quad (23)$$

where the various parameters are chosen so that $N > 0$, $z_0 > 0$, and $a > 0$, the latter being aimed at avoiding singularity at $x = 0$ and similarly at $(z = 0, t = 0)$.

As noted in the Introduction, the above can be regarded as the 1D Cartesian versions of the axially symmetric functions discussed in [19] and there related to the splash pulses [13–16] with inherent exponent $\delta > \frac{1}{2}$. Then, following the terminology adopted in [19], one may refer to (23) as the "fundamental" *Hermite-Lorentzian* solution of the 2D wave equation.

As is well known, the paraxial limit of (23) is obtained by replacing σ by $2z$ [31–33]. Also, a simple interchange of σ and τ in (23) yields an alternative solution of (2) as well as, with $\sigma \to 2z$, of the relevant paraxial limit.

Figure 2 shows the surface plots and the corresponding contour plots of the amplitude of the Lorentzian-like solution (23) for $N = 0.1$, 0.3, 0.5, 1 and $z_0 = 10^{-2}$ cm and $a = 2{\cdot}10^3$ cm. The graphs refer to the pulse center $z_c = ct = 0$, so that $z = \tau$ is just the distance along the direction of propagation away from the pulse center; in addition, the maximum in each plot is normalized to unity. The plots for $N > 1$ look quite similar to that for $N = 1$, with the central peak being compressed along the x direction when increasing N; in other words, the 8-like shape in the (τ, x) plane displayed by the contour plots relevant to $N = 1$ comes to squeeze up along the x direction with increasing N.

Evidently the localization of $\phi_{0,\,N}$ along the longitudinal and transverse directions is controlled by the length parameters z_0 and a.

In particular, let us illustrate the behavior of $\phi_{0,\,N}$ at the pulse center $z = z_c = ct$. We see that the squared amplitude $|\phi_{0,\,N}|^2$ at $z = z_c$ behaves with x and z as

$$\left|\phi_{0,\,N}(x, z = ct)\right|^2 = \frac{1}{4^N z_0} \frac{1}{\left[z^2 + \frac{a^2}{4}\left(1 + \frac{x^2}{a z_0}\right)^2\right]^N}, \tag{24}$$

which conveys $\frac{a}{2}$ and $\sqrt{a z_0}$ as a sort of characteristic lengths for the variations of $\phi_{0,\,N}$ (at $z = z_c$) along the z and x directions, respectively. Until $z \lesssim \frac{a}{2\sqrt{N}}$ the pulse shape does not vary much with z, being $|\phi_{0,N}(x, z = ct \lesssim \frac{a}{2\sqrt{N}})|^2 \sim \frac{1}{z_0 a^{2N}} \frac{1}{(1+\frac{x^2}{a z_0})^{2N}}$. So, the amplitude decrease from $x = 0$ to $x \lesssim \sqrt{\frac{a z_0}{N}}$ mantains roughly within a factor 2. Then, for $z > \frac{a}{2\sqrt{N}}$ the amplitude (at $z = z_c$) decays like z^{-N}. Therefore, for values of $0 < N < 1$, we might observe a missilelike behavior [34, 35] of the corresponding $\phi_{0,\,N}$ (see Fig. 5 below).

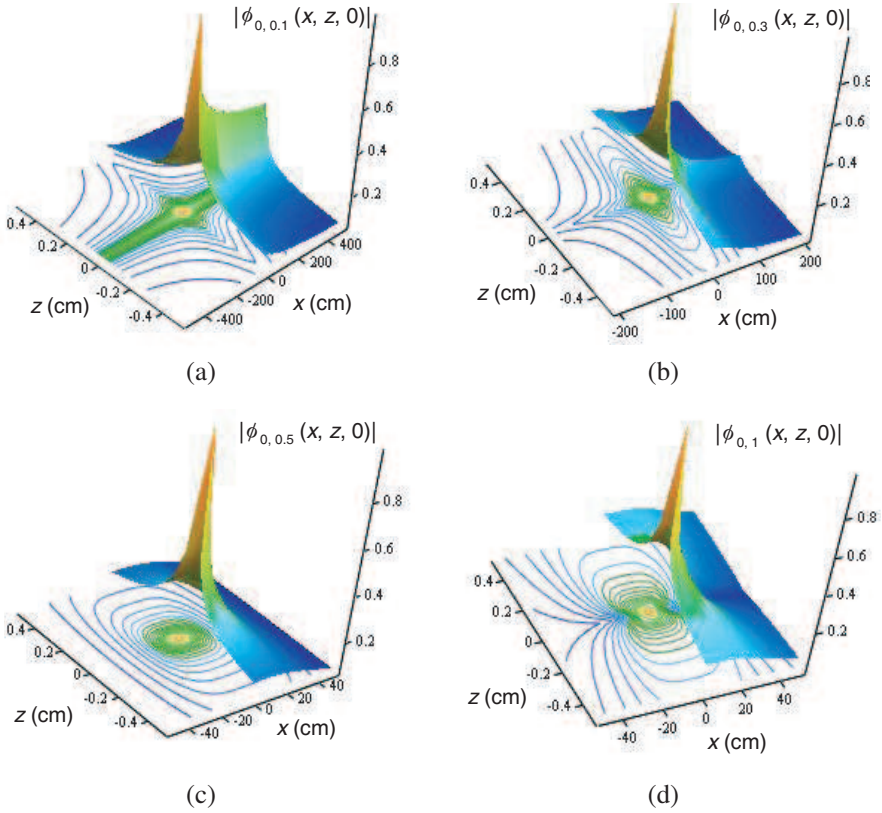

Figure 2. Amplitude $|\phi_{0,N}|$ vs. x and τ at the pulse center $z_c = ct = 0$ for $z_0 = 10^{-2}$ cm, $a = 2 \cdot 10^3$ cm, and (a) $N = 0.1$, (b) $N = 0.3$, (c) $N = 0.5$, (d) $N = 1$.

It is well known that "higher-order" solutions of the wave Equation (2) can be generated from a given solution (the "fundamental" one) by applying to the latter the derivative operator

$$D^{(m)} = \frac{\partial^h}{\partial x^h} \frac{\partial^j}{\partial \sigma^j} \frac{\partial^l}{\partial \tau^l}, \quad m = h + j + l$$

for any nonnegative integers (actually also nonnegative real), just because the differential operator in Equation (2) commutes with $D^{(m)}$.

In particular, if $v(x, \sigma, \tau)$ solves (2), so does also $v_h(x, \sigma, \tau) = \frac{\partial^h}{\partial x^h} v(x, \sigma, \tau)$ for any non-negative real value of h. Accordingly, from (23) we may generate further solutions of the 2D wave equation

as

$$\begin{aligned}\phi_{n,\,N}(x,z,t) &= \frac{\partial^n}{\partial x^n}\phi_{0,\,N}(x,z,t)\\ &= \frac{(-)^n N^{\frac{n}{2}}}{(\tau-iz_0)^{\frac{n+1}{2}}(\sigma+ia)^{N+\frac{n}{2}}}\Phi_n^{(N)}\left(X_N(x,z,t)\right). \quad (25)\end{aligned}$$

Here, $\Phi_n^{(N)}(\cdot)$ denotes the HLFs discussed in the previous section, whose argument is

$$X_N(x,z,t) = \sqrt{\frac{N}{(\sigma+ia)(\tau-iz_0)}}x, \quad (26)$$

where the branches of the square root can be chosen arbitrarily. One may refer to the above as *Hermite-Lorentzian* solutions of order n (and parameter N) of the homogeneous 2D wave Equation (2).

Although we consider here only non-negative integer values of n, any non-negative real value is allowed as well; in that case, one should deal with the expression for the relativistic Hermite polynomials in terms of the proper Gauss hypergeometric function, deducible from (8). We might talk of *fractional order Hermite-Lorentzian* solutions of the 2D wave equation. Such a case is beyond the purposes of the present discussion.

The $\phi_{n,\,N}$'s combine the multi-Lorentzian-like factor $\frac{1}{\sqrt{\tau-iz_0}}(\sigma+ia+\frac{x^2}{\tau-iz_0})^{-N-n} = (\sigma+ia+\frac{x^2}{\tau-iz_0})^{-n}\phi_{0,\,N}(x,z,t)$ with the x-dependent polynomial component comprising also the σ- and τ-dependent factor, i.e., $\frac{(\sigma+ia)^{\frac{n}{2}}}{(\tau-iz_0)^{\frac{n}{2}}}H_n^{(N)}(X_N(x,z,t))$. Hence, their behavior results from the combination of those of both components.

Clearly the Lorentzian-like factor behaves as previously discussed, with the relative characteristic lengths being properly scaled to account for the further presence of the integer n in the exponent.

On the other hand, we see that the argument $X_N(x,z,t)$ of the RHP in (25) is in general complex, and hence the behavior of the polynomial component in (25) may significantly differ from that of the same polynomial with real argument. In particular, X_N becomes real at $z=ct=0$, being $X_N(x,z=ct=0)=\sqrt{\frac{N}{az_0}}x$, whilst in general at the pulse center $z=ct$ it turns out to be

$$X_N(x,z=ct) = \sqrt{\frac{iN}{z_0(2z+ia)}}x. \quad (27)$$

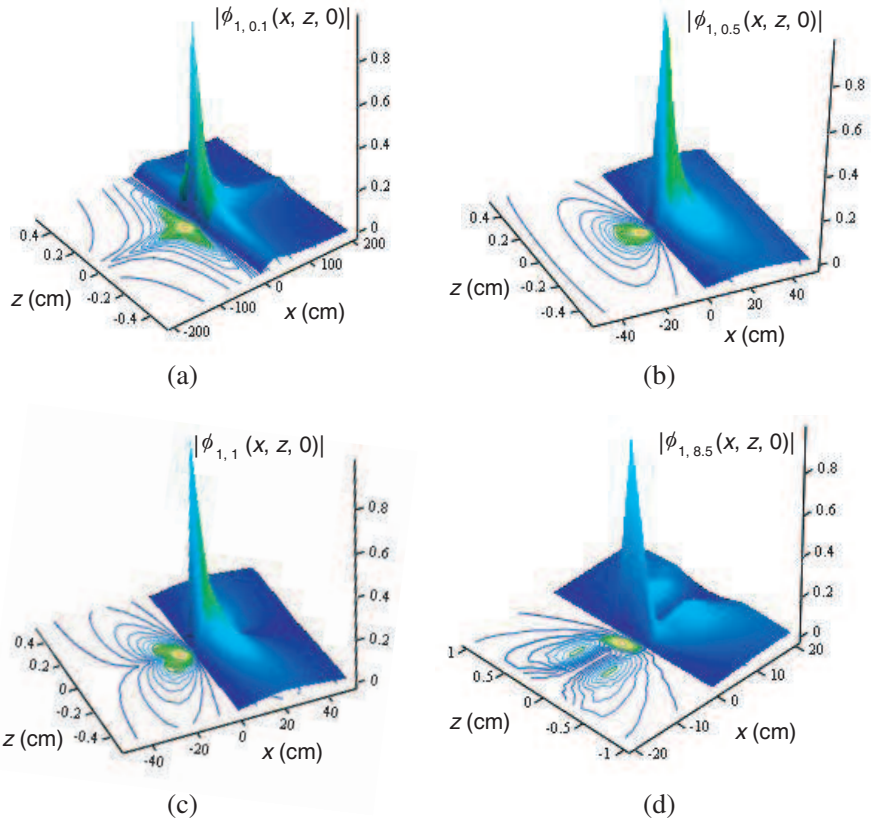

Figure 3. Amplitudes $|\phi_{1,N}|$ vs. x and τ at the pulse center $z_c = 0$ for (a) $N = 0.1$, (b) $N = 0.5$, (c) $N = 1$ and (d) $N = 8.5$. In all cases, $z_0 = 10^{-2}$ cm and $a = 2 \cdot 10^3$ cm.

Then, if $z \lesssim \frac{a}{2\sqrt{N+n}}$ the above comes to be rather well approximated by the real z-independent expression

$$X_N \left(x, z = ct \lesssim \frac{a}{2\sqrt{N+n}} \right) \simeq \sqrt{\frac{N}{z_0 a}} x. \tag{28}$$

Likewise, the multiplying factor remains almost constant to $\frac{i^{\frac{n}{2}}(2z+ia)^{\frac{n}{2}}}{z_0^{\frac{n}{2}}} \sim (-\frac{a}{z_0})^{\frac{n}{2}}$. Further, until $x \lesssim \sqrt{\frac{az_0}{N+n}}$, $X_N < 1$, so that one may approximate the polynomial factor by the relevant lowest-order

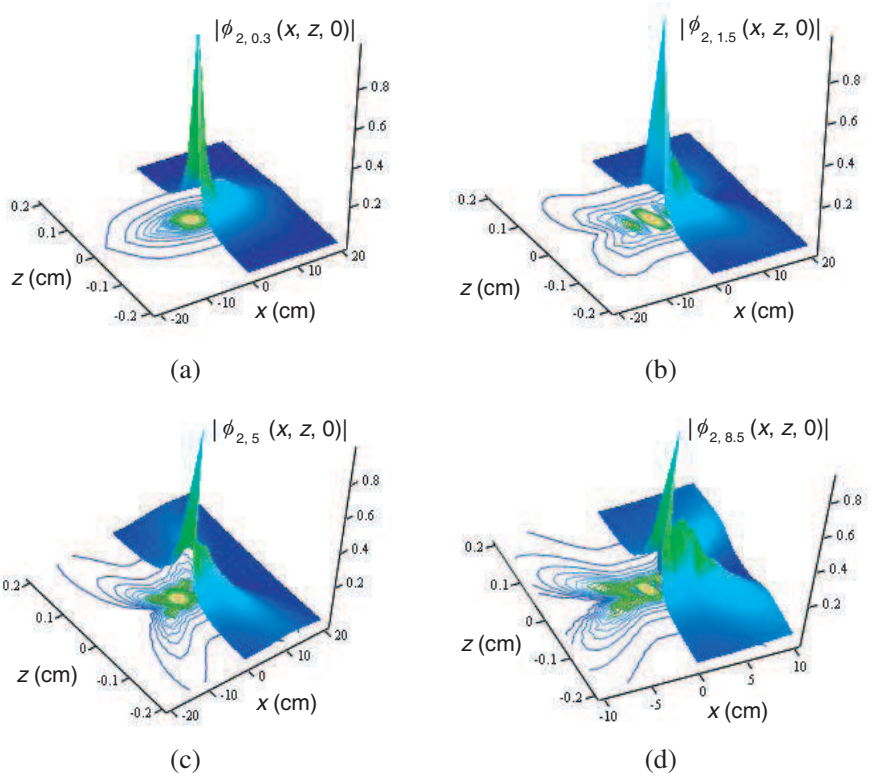

Figure 4. Amplitudes $|\phi_{2,N}|$ vs. x and τ at the pulse center $z_c = 0$ for (a) $N = 0.3$, (b) $N = 1.5$, (c) $N = 5$ and (d) $N = 8.5$. In all cases, $z_0 = 10^{-2}$ cm and $a = 2 \cdot 10^3$ cm.

power, thus yielding for the squared amplitude the expression

$$\left|\phi_{n,N}\left(x \lesssim \sqrt{\frac{az_0}{N+n}}, z = ct \lesssim \frac{a}{2\sqrt{N+n}}\right)\right|^2$$
$$\sim \begin{cases} \dfrac{4^n\left[\left(\frac{1}{2}\right)_m (N)_m\right]^2}{z_0^{n+1} a^{2N+n}} \dfrac{1}{\left(1+\frac{x^2}{az_0}\right)^{2N+2n}}, & n = 2m \\ \dfrac{4^n\left[n(N+m)\left(\frac{1}{2}\right)_m (N)_m\right]^2}{z_0^{n+1} a^{2N+n}} \dfrac{x^2/az_0}{\left(1+\frac{x^2}{az_0}\right)^{2N+2n}}, & n = 2m+1. \end{cases} \quad (29)$$

In contrast, for $x > \sqrt{Naz_0}$ the polynomials might be approximated by the relevant highest powers thus yielding the

expression

$$\left|\phi_{n,\,N}\left(x>\sqrt{Naz_0}, z=ct\lesssim\frac{a}{2\sqrt{N+n}}\right)\right|^2\sim\frac{[(2N)_n]^2}{z_0a^{2N+2n}}\frac{\left(x/\sqrt{az_0}\right)^n}{\left(1+\frac{x^2}{az_0}\right)^{2N+2n}}. \quad (30)$$

where the power x^n mitigates the descending trend of the multi-Lorentzian factor $(1+\frac{x^2}{az_0})^{-2N-2n}$.

Figures 3 and 4 show the surface plots and the corresponding contour plots of the amplitudes $|\phi_{n,\,N}|$ vs. x and τ at the pulse center $z_c=0$ respectively for $n=1$ and $n=2$ and different values of N. In all cases, $z_0=10^{-2}$ cm and $a=2\cdot10^3$ cm. Again, the maximum in each plot is normalized to unity.

We see that the shape of the plots changes rather significantly with N. In fact, for $n=1$ we observe, as expected, two identical lobes at each side of the central nodal line $x=0$. For $N=0.1$ the contour plot for each lobe exhibits an irregular rhombo-like shape, whereas an overall 8-like shape in the (x,τ) plane is in contrast obtained for the contour plot relevant to $N=0.5$. Then, a butterfly-like shape pertains to the case $N=1$, which shape is further deformed with increasing N, two lateral lobes more strongly emerging to each side with increasing N.

Likewise, for $n=2$ one gets an almond-shaped contour plot with a predominant central lobe for $N\leq1$. The lateral lobes separate from the central one, becoming more evident indeed with increasing N up to $N\lesssim2.5$. Then, for $N>2.5$ they come to be re-absorbed in the central lobe, which so displays a more complex structure, with an overall four-petal flower-like appearance of the relevant contour plots.

Similar behaviors are observed for higher values of n, respectively odd and even, although the effect of N becomes evident for even higher N with increasing n.

Finally, in Fig. 5, we have plotted the peak amplitudes of the $\phi_{n,N}$'s at the pulse center $z=ct$ vs. z for some values of n and N with the parameters z_0 and a being set as before to $z_0=10^{-2}$ cm and $a=2\cdot10^3$ cm. The symbol x^* appearing in the labels of the vertical axis in the plots in Parts (c) and (d) denote the value of x, $x^*(n,N)$, at which $|\phi_{n,\,N}(x,z=ct)|$ is maximum. Such maxima occur at $x^*=0$ for even n, like $n=0$ and $n=2$ to which the graphs in Frames (a) and (b) of the figure pertain. In contrast, we found that the x^*'s accomodate rather well according to the relation

$$x^*(n=1,N)[\text{cm}]\simeq\frac{4.45}{(1.5N+1)^{0.55}},$$

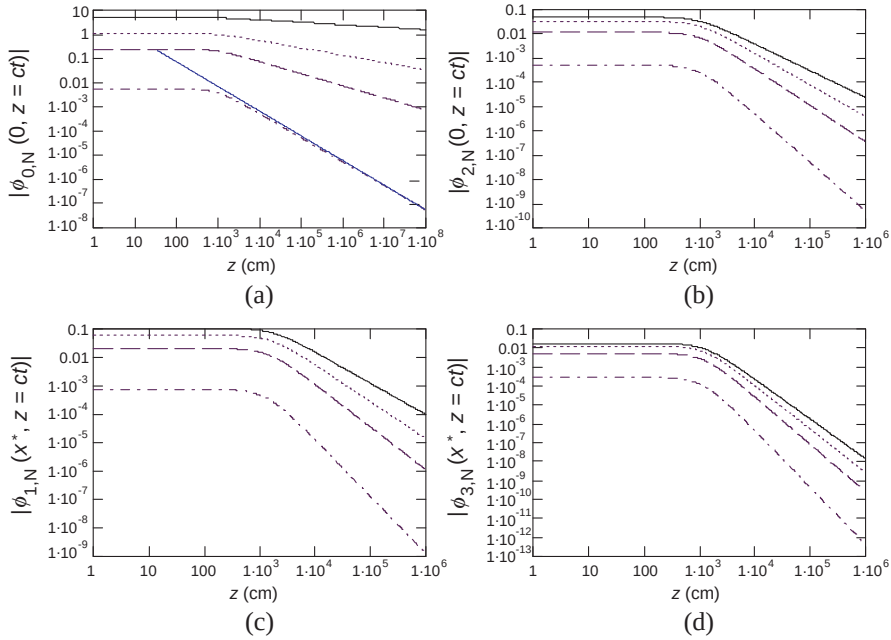

Figure 5. Peak amplitudes $|\phi_{n,N}(x^*, z = ct)|$ vs. z for $N = 0.1$ (solid line), 0.3 (dotted line), 0.5 (dashed line), 1 (dash-dotted line) and (a) $n = 0$, (b) $n = 2$, (c) $n = 1$ and (d) $n = 3$ with $z_0 = 10^{-2}$ cm, $a = 2 \cdot 10^3$ cm.

for $n = 1$, and to

$$x^*(n = 3, N)[\text{cm}] \simeq \frac{4.45}{(1.5N + 3)^{0.7}},$$

for $n = 3$. We recall that the odd n amplitudes at $z = ct$ exhibit a two main lobes structure.

The straight line in the plot of Part (a) of the figure (relevant to $n = 0$) reproduces a z^{-1}-like decay, which as expected rules the amplitude for $N = 1$ at large values of z : $z > 10^5$ cm. Evidently the other plots in the same frames display a decay for large z slower than z^{-1}. Such a decay, which amounts to a power decay slower than the usual z^{-2}, is reported in the literature as missilelike [34, 35]; it attracted interest for possible applications in the transmission of information, which so might be very difficult to intercept or jam [34, 35]. As to the plots in the other frames, we note that for $n = 1$ and $n = 2$, we detect a peak amplitude decay respectively of $\sim z^{-0.91}$ and $\sim z^{-0.95}$ at $N = 0.1$, whilst decays roughly as or faster than z^{-1} pertain to the

peak amplitudes for $N > 0.1$. Finally, for $n = 3$ a decay faster than z^{-1} is displayed by the peak amplitudes for all the values of N considered in the figure (for instance, as $\sim z^{-1.75}$ at $N = 0.1$). Evidently, these considerations would gain a further practical interest once the practical launchability of the concerned wave functions could be demonstrated, but, as previously stressed, we will not dwell here on such an issue.

Before closing the section, we wish to note that the above introduced solutions of the 2D wave equation frame within the class of Courant-Hilbert solutions [36], which in general write as

$$u(x, y, z, t) = hf(\theta). \tag{31}$$

The *waveform* f is an arbitrary function of a single variable with continuous partial derivatives, whilst the *phase* function $\theta(x, y, z, t)$ and the *attenuation* (or *distortion*) factor $h(x, y, z, t)$ are fixed functions. In particular, θ is any solution of the space-time eikonal equation $(\theta_x)^2 + (\theta_y)^2 + (\theta_z)^2 - (\theta_{ct})^2 = 0$.

Evidently, in the case of the 2D solutions $\phi_{n,N}$'s, the phase

$$\theta(x, z, t) = \sigma + \frac{x^2}{\tau - iz_0}, \tag{32}$$

is just the 2D version of the Bateman-Hillion phase [4, 7], whereas the relevant waveform f shapes as the power function $f_{n,N}(\theta) = (\theta + ia)^{-N-n}$ and the attenuation factor is $h_{n,N}(x, z, t) \propto \frac{(\sigma+ia)^{\frac{n}{2}}}{(\tau-iz_0)^{\frac{n+1}{2}}} H_n^{(N)}(X_N(x, z, t))$.

4. THE RELATIVISTIC HERMITE POLYNOMIALS AND THE 3D WAVE EQUATION

As recalled in Introduction, there are definite rules to construct solutions of the 3D wave equation from those of the 2D one. In particular, we consider here the solutions of the 3D wave equation, $u_{n,N}(x, y, z, t)$, obtained from the above introduced $\phi_{n,N}$'s according to the transformation (3), which so yields

$$u_{n,N}^{(\pm)}(x, y, z, t) = (x \pm iy)^{-\frac{1}{2}} \phi_{n,N}(r, z, t) = r^{-\frac{1}{2}} e^{\mp \frac{i}{2}\varphi} \phi_{n,N}(r, z, t), \tag{33}$$

where $\phi_{n,N}$ is given in Equation (25) and r, φ denote polar coordinates in the x-y plane: $r = \sqrt{x^2 + y^2}$, $\varphi = \arctan(\frac{y}{x})$.

Again, the interchange of σ and τ in (33) provide alternative solutions of (1). Also, as previously recalled, replacing $\sigma \to 2z$ in

the wave functions yields the expressions of the corresponding pulsed beams [31–33].

Evidently for any n the $u_{n,N}^{(\pm)}$'s are not axisymmetric, even though their amplitudes are.

The $u_{n,N}^{(\pm)}$'s as well belong to the class (31) of Courant-Hilbert solutions of the wave equation [36]. The relevant phase $\theta(x,y,z,t)$ is just the Bateman-Hillion axisymmetric phase, i.e., (32) with r in place of x, the waveform shapes as before as $f_{n,N}(\theta) = (\theta + ia)^{-N-n}$, whereas the attenuation factor exhibits now the factor $(x \pm iy)^{-\frac{1}{2}}$, i.e., $h_{n,N}^{(\pm)}(x,y,z,t) \propto (x \pm iy)^{-\frac{1}{2}} \frac{(\sigma+ia)^{\frac{n}{2}}}{(\tau - iz_0)^{\frac{n+1}{2}}} H_n^{(N)}(X_N(r,z,t))$.

It is just due to such a factor that the $u_{n,N}^{(\pm)}$'s might present the fixed curve of singularities ($x = 0$, $y = 0$). This undeniably occurs for even n's, whilst it is easy to see that for odd n's $h_{n,N}^{(\pm)}(x,y,z,t) \xrightarrow[x\to 0,\, y\to 0]{} 0$. To avoid the singularity occurring for even n's, one may take $\frac{\partial}{\partial(x+iy)} u_{n,N}^{(+)}$ and $\frac{\partial}{\partial(x-iy)} u_{n,N}^{(-)}$ when $n = 2m$. As we will see in the following, this amounts to consider only the odd-order forms of (33), i.e., $u_{2m+1,N}^{(\pm)}$.

Then, on account of the above illustrated behavior of the amplitudes $|\phi_{n,N}|$ at the pulse center (see Equations (29) and (41)), we see that

$$\left| u_{n,N}^{(\pm)} \left(x, y, z = ct \lesssim \frac{a}{2\sqrt{N+n}} \right) \right|^2 \sim \begin{cases} \frac{4^n \left[\left(\frac{1}{2}\right)_m (N)_m \right]^2}{z_0^{n+1} a^{2N+n}} \frac{1/r}{\left(1+\frac{r^2}{az_0}\right)^{2N+2n}}, & n = 2m \\ \frac{4^n \left[n(N+m) \left(\frac{1}{2}\right)_m (N)_m \right]^2}{z_0^{n+\frac{3}{2}} a^{2N+n+\frac{1}{2}}} \frac{r/\sqrt{az_0}}{\left(1+\frac{r^2}{az_0}\right)^{2N+2n}}, & n = 2m+1 \end{cases} \tag{34}$$

for $r \lesssim \sqrt{\frac{az_0}{N+n}}$, whereas for $r > \sqrt{Naz_0}$

$$\left| u_{n,N}^{(\pm)} \left(x, y, z = ct \lesssim \frac{a}{2\sqrt{N+n}} \right) \right|^2 \sim \frac{[(2N)_n]^2}{z_0^{\frac{3}{2}} a^{2N+2n+\frac{1}{2}}} \frac{\left(r/\sqrt{az_0}\right)^{n-1}}{\left(1+\frac{r^2}{az_0}\right)^{2N+2n}}. \tag{35}$$

As an example, Fig. 6 shows the contour plots of the amplitudes $|u_{n,N}^{(\pm)}|$ vs. r and z at the pulse center $z_c = 0$ for some values of the

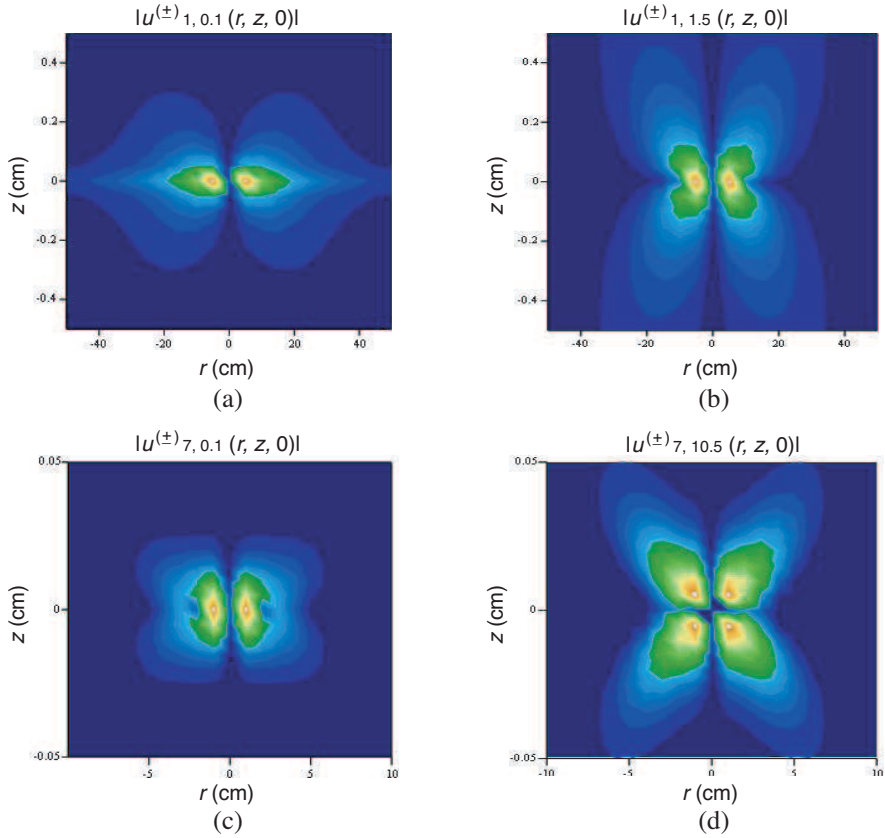

Figure 6. Contour plots of the amplitudes $|u^{(\pm)}_{n,N}|$ vs. r and z at $t = 0$ for (a) $n = 1$, $N = 0.1$, (b) $n = 1$, $N = 1.5$, (c) $n = 7$, $N = 0.1$ and (d) $n = 7$, $N = 10.5$. In all cases, $z_0 = 10^{-2}$ cm and $a = 2 \cdot 10^3$ cm.

parameter N and the order n (in particular odd according to the above considerations).

A numerical analysis of the cases in the figure has shown that the relative r-z amplitude distributions remain almost unaltered, apart from a sort of breathing (a smooth sequence of broadening and focusing more evident along the z-direction at a rather irregular rate), up to $t \approx 10^{-9} - 10^{-8}$ s (basically depending on n and N, for the fixed values of z_0 and a as in the cases of the figure). Then, such distributions start to change rather rapidly developing two more or less subtle "walls" also displaying a somewhat articulated structure.

Let us note that, as in the previous figures, the values of the free parameters z_0 and a have been set to $z_0 = 0.01$ cm and $a =$

$2 \cdot 10^3$ cm and so $z_0 \ll a$. Therefore, according to the analysis presented in [17, 18], where the electromagnetic vector fields generated by the wave function $s_1(x, y, z, t) = \frac{1}{(\sigma+ia)(\tau-iz_0)+r^2}$, taken as a Hertz potential oriented both parallel [17] and orthogonal [18] to the z-direction have been studied in detail, the frames in the figures pertain to the paraxial regime ($z_0 \ll a$). So, it may be interesting to compare the r-z amplitude behavior in the case $z_0 \ll a$ and in the case $z_0 \approx a$. Fig. 7 shows indeed the r-z contour plots of the amplitudes $|u^{(\pm)}_{n,N}|$ for $n = 5$ and $N = 2.1$ at $t = 0$ and $t > 0$ for two sets of values of z_0 and a, i.e., as before, $z_0 = 0.01$ cm and $a = 2 \cdot 10^3$ cm ($z_0 \ll a$) and $z_0 = 10$ cm and $a = 20$ cm ($z_0 \approx a$).

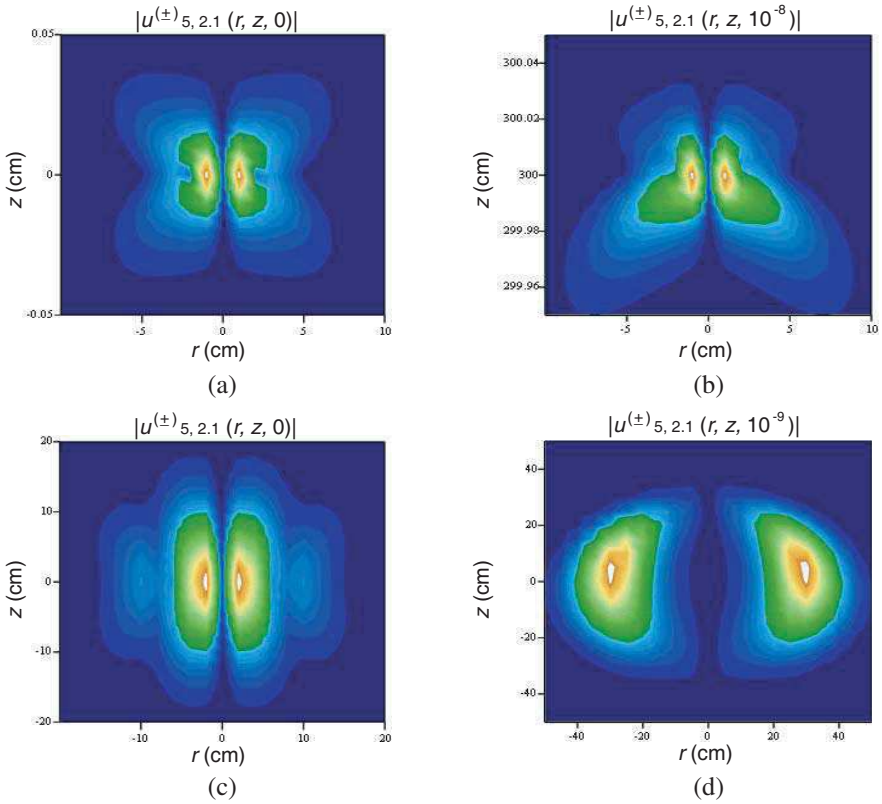

Figure 7. Contour plots of the amplitudes $|u^{(\pm)}_{5,2.1}|$ vs. r and z relative to $z_0 = 10^{-2}$ cm and $a = 2 \cdot 10^3$ cm at (a) $t = 0$ and (b) $t = 10^{-8}$ s and to $z_0 = 10$ cm and $a = 20$ cm at (c) $t = 0$ and (d) $t = 10^{-9}$ s.

5. HERMITE-LORENTZIAN WAVE FUNCTIONS: RELATION TO THE LAGUERRE-LORENTZIAN WAVE FUNCTIONS

As mentioned earlier, the splash pulses (6) are solutions of the 3D wave equation. In particular, considering exponents $\delta > 0$, one could understand the relevant splash pulses as the 3D counterpart of the $\phi_{0,N}$'s with the cartesian coordinate x replaced by the radial one r, and the further multiplication by the factor $\frac{1}{\sqrt{\tau - iz_0}}$. In symbols, with $\delta = N$ in (6) one has

$$s_N(x, y, z, t) = \frac{1}{\sqrt{\tau - iz_0}} \phi_{0,N}(r, z, t). \tag{36}$$

Of course, in order that the above could convey a rule to construct solutions of the 3D wave equation from those of the 2D wave equation, namely,

$$\phi(x, z, t) \to v(x, y, z, t) = \frac{1}{\sqrt{\tau - iz_0}} \phi(r, z, t), \tag{37}$$

the 2D solution $\phi(x, z, t)$ must satisfy the equation

$$\left[\frac{\partial}{\partial x} - \frac{2x}{\tau - iz_0} \frac{\partial}{\partial \sigma} \right] \phi(x, z, t) = 0. \tag{38}$$

The above is evidently satisfied by the $\phi_{0,N}$'s for any N, and hence by (37) one gets the splash pulses (36).

On passing we may note that Equation (38) is satisfied by the 2D Gaussian pulse $\phi_{\mathrm{G}}(x, z, t) = \frac{1}{\sqrt{\tau - iz_0}} e^{ik\theta(x,z,t)}$ as well as by the 2D modified-power-spectrum (MPS) pulse $\phi_{\mathrm{MPS}}(x, z, t) = \frac{1}{\sqrt{\tau - iz_0}} \frac{1}{(\theta + ia)^q} e^{ik\theta(x,z,t)}$, from which indeed through (37) one respectively gets the 3D Gaussian and MPS pulses [24], the latter combining both the Gaussian and splash-pulse waveforms.

As previously recalled, the splash pulses have been reconsidered in [19] in the form

$$v_{0,N}(r, z, t) = \frac{1}{\tau - iz_0} \left(\sigma + ia + \frac{r^2}{\tau - iz_0} \right)^{-N - \frac{1}{2}}, \tag{39}$$

i.e., for exponents $\delta > \frac{1}{2}$. This was functional to the possibility of conveniently relating some higher-order solutions $v_{n,l,N}(x, y, z, t)$ to the RLPs (20). Such solutions are generated by repeatedly acting on (39)

by the operators $\widehat{\mathcal{L}}_{\pm}$

$$\widehat{\mathcal{L}}_{\pm}(x,y) = \frac{\partial}{\partial x} \pm i\frac{\partial}{\partial y} = e^{\pm i\varphi}\left(\frac{\partial}{\partial r} \pm \frac{i}{r}\frac{\partial}{\partial \varphi}\right) = 2\frac{\partial}{\partial(x \mp iy)}. \tag{40}$$

Since $\widehat{\mathcal{L}}_{+}\widehat{\mathcal{L}}_{-} = \widehat{\mathcal{L}}_{-}\widehat{\mathcal{L}}_{+} = \frac{\partial^2}{\partial x^2} + \frac{\partial^2}{\partial y^2}$ and $[\frac{\partial}{\partial\sigma,\tau}, \widehat{\mathcal{L}}_{\pm}] = 0$, it is evident that

$$v_{n,l,N}(x,y,z,t) = \widehat{\mathcal{L}}_{+}^{n}\widehat{\mathcal{L}}_{-}^{n+l}v_{0,N}(r,z,t) \tag{41}$$

is a solution of the 3D wave equation for values of the integers n and l, respectively addressed as radial and angular indices, such that $n \geq 0$ and $l \geq -n$. Specifically, in [19] the axisymmetric solutions generated from the scheme (41) with $l = 0$, in which case: $\widehat{\mathcal{L}}_{+}^{n}\widehat{\mathcal{L}}_{-}^{n} = [\nabla_r^2]^n$, have been discussed in detail, and there related, as mentioned earlier, to the RLPs, which in fact act as modulating factors of the axisymmetric Lorentzian-like wave functions (39), whose exponent is further increased to $N + 2n + \frac{1}{2}$.

In the same vein, we may ask whether the above introduced *Hermite-Lorentzian* solutions of the 3D wave equation $u_{n,N}^{(\pm)}(x,y,z,t)$, being obtained through (3) from the higher-order *Hermite-Lorentzian* solutions $\phi_{n,N}(x,z,t)$ of the 2D wave equation, might be understood as higher-order solutions relatively to certain fundamental ones, which could reasonably be guessed to be $u_{0,N}^{(\pm)}(x,y,z,t) = (x \pm iy)^{-\frac{1}{2}}\phi_{0,N}(r,z,t)$. In other words, we may ask whether it is possible to identify a sort of generation scheme for the $u_{n,N}^{(\pm)}$'s as

$$u_{j(m),N}^{(\pm)}(x,y,z,t) = \widehat{\mathcal{V}}_{\pm}^{m}\,\mathfrak{u}_{0,N}^{(\pm)}(x,y,z,t),$$

for some fundamental solutions $\mathfrak{u}_{0,N}^{(\pm)}(x,y,z,t)$. The order j of the resulting functions may in general depend in some way on the power m (> 0), to which the generation operators $\widehat{\mathcal{V}}_{\pm}$ (practically, symmetry operators of the wave equation) are rised up.

In this connection, it is easy to verify that

$$\begin{aligned} &\widehat{\mathcal{L}}_{+}u_{n,N}^{(+)} = u_{n+1,N}^{(-)}, \qquad \widehat{\mathcal{L}}_{-}u_{n,N}^{(-)} = u_{n+1,N}^{(+)}, \\ &\widehat{\mathcal{L}}_{+}\widehat{\mathcal{L}}_{-}u_{n,N}^{(+)} = u_{n+2,N}^{(+)}, \quad \widehat{\mathcal{L}}_{+}\widehat{\mathcal{L}}_{-}u_{n,N}^{(-)} = u_{n+2,N}^{(-)}. \end{aligned} \tag{42}$$

Then, considering the two sets of functions $u_{n,N}^{(+)}$ and $u_{n,N}^{(-)}$ we may say that elements in the same set are connected by steps of 2 in the relative orders by the transverse Laplacian $\widehat{\mathcal{L}}_{+}\widehat{\mathcal{L}}_{-}$, whereas elements in

the two sets are connected by steps of 1 in the relative orders by $\widehat{\mathcal{L}}_+$ and $\widehat{\mathcal{L}}_-$, respectively bridging the $u_{n,N}^{(+)}$'s to the $u_{n,N}^{(-)}$'s and vice versa. So, as noted earlier, taking the solutions $\widehat{\mathcal{L}}_+ u_{2m,N}^{(+)}$ and $\widehat{\mathcal{L}}_- u_{2m,N}^{(-)}$ one can avoid the singularity associated with the even-order forms of (33) simply because so doing one picks up only the odd-order forms of (33).

According to (42), we may generate elements in each set applying $\widehat{\mathcal{L}}_+\widehat{\mathcal{L}}_-$ to $u_{0,N}^{(\pm)}$ and to $u_{1,N}^{(\pm)}$, which so turn respectively into the even and odd order solutions $u_{2m,N}^{(\pm)}$ and $u_{2m+1,N}^{(\pm)}$. In other word, the even and odd order solutions, $u_{2m,N}^{(\pm)}$ and $u_{2m+1,N}^{(\pm)}$, arise from different paths, one originating from $u_{0,N}^{(\pm)}$ the other from $u_{1,N}^{(\pm)}$:

$$\left[\widehat{\mathcal{L}}_+\widehat{\mathcal{L}}_-\right]^m u_{0,N}^{(\pm)} = u_{2m,N}^{(\pm)}, \quad \left[\widehat{\mathcal{L}}_+\widehat{\mathcal{L}}_-\right]^m u_{1,N}^{(\pm)} = u_{2m+1,N}^{(\pm)}. \tag{43}$$

Furthermore, a more compact scheme can be identified, which will also clarify the link of the $u_{n,N}^{(\pm)}$'s with the 3D solution (39) and its higher order versions (41), considered in detail, as already mentioned, in [19].

In fact, taking into account the relations (19) between the RHPs and the RLPs and the formal expressions

$$\widehat{\mathcal{L}}_+^n\widehat{\mathcal{L}}_-^{n+l}\left(1+\frac{r^2}{N}\right)^{-N-\frac{1}{2}} = (-)^{n+l}2^{2n+l}n!\frac{\Gamma\left(N+\frac{1}{2}+n+l\right)}{\Gamma\left(N+\frac{1}{2}\right)N^{n+l}}r^l e^{-il\varphi}L_n^{(l,N)}\left(r^2\right)$$
$$\left(1+\frac{r^2}{N}\right)^{-N-2n-l-\frac{1}{2}}, \quad n\geq 0,\, l\geq -n, \tag{44}$$

after some algebra we end up with the generation scheme for the $u_{n,N}^{(\pm)}$'s

$$u_{n,N}^{(\pm)}(x,y,z,t) = \widehat{\mathcal{L}}_{\mp}^{\frac{n}{2}}\widehat{\mathcal{L}}_{\pm}^{\frac{n-1}{2}} v_{0,N}(r,z,t), \tag{45}$$

involving the splash pulses (39).

Evidently, the above for $n=0$ allows one to relate the rule (3) in the case of the $v_{0,N}$'s to the symmetry operators $\widehat{\mathcal{L}}_\pm$ (rised to $\pm\frac{1}{2}$) of the wave equation.

We note that according to whether the order n is even or odd the power $\pm\frac{1}{2}$ of the operators $\widehat{\mathcal{L}}_\pm$ is involved in (45). The effect of $\widehat{\mathcal{L}}_\pm^{\pm\frac{1}{2}}$ can be proved to be in accord with the general relation (44), on account of the operational rule for negative powers of operators [37]

$$\widehat{\mathcal{A}}^{-p} = \frac{1}{\Gamma(p)}\int_0^\infty ds s^{p-1}e^{-s\widehat{\mathcal{A}}}, \quad p\in\mathbb{R}^+.$$

The above yields in fact for the operators of our concern the expression

$$\widehat{\mathcal{L}}_{\pm}^{-\frac{1}{2}} = \frac{1}{\Gamma\left(\frac{1}{2}\right)} \int_0^\infty ds s^{-\frac{1}{2}} e^{-s\widehat{\mathcal{L}}_{\pm}},$$

which explicitly amounts to

$$\widehat{\mathcal{L}}_{\pm}^{-\frac{1}{2}} \psi(x,y) = \frac{1}{\sqrt{\pi}} \int_0^\infty ds s^{-\frac{1}{2}} \psi(x-s, y \mp is),$$

and hence to

$$\widehat{\mathcal{L}}_{\pm}^{\frac{1}{2}} \psi(x,y) = \widehat{\mathcal{L}}_{\pm} \widehat{\mathcal{L}}_{\pm}^{-\frac{1}{2}} \psi(x,y) = \frac{1}{\sqrt{\pi}} \int_0^\infty ds s^{-\frac{1}{2}} \left[\widehat{\mathcal{L}}_{\pm} \psi\right](x-s, y \mp is).$$

The direct application of the above rules to $v_{0,N}(r,z,t)$ yields the relations (45).

Interestingly, the *Hermite-Lorentzian* solutions of the 3D wave equation appear to be generated by repeated applications of half-integer powers of the operators $\widehat{\mathcal{L}}_{\pm}$ to the fundamental axisymmetric Lorentzian-like solution — or splash pulse — $v_{0,N}$. In other words, we may say that the $u_{n,N}^{(\pm)}$'s can be constructed by the same scheme (41) through which the Laguerre-Lorentzian solutions are generated, but with $l = \pm\frac{1}{2}$, the orders of the involved RHPs in the resulting functions being accordingly odd or even. In a sense, the $u_{n,N}^{(\pm)}$'s can be regarded as higher-order Laguerre-Lorentzian solutions of the 3D wave equation (or, higher-order splash pulses) corresponding to fractional azimuthal orders, specifically $\pm\frac{1}{2}$.

Needless to say, relations (45) are in accord with (42). Furthermore, as conveyed by (42) and (43), applying $\widehat{\mathcal{L}}_{+}$, $\widehat{\mathcal{L}}_{-}$ or $\widehat{\mathcal{L}}_{+}\widehat{\mathcal{L}}_{-}$ yields further solutions of the wave equation. Interestingly, one can get "compact" forms through the schemes

$$\begin{aligned} \widehat{\mathcal{L}}_{+}^{m} u_{0,N}^{(+)} &\longrightarrow \frac{(x+iy)^m}{(\tau - iz_0)^m} u_{0,N+m}^{(+)}, \\ \widehat{\mathcal{L}}_{-}^{m} u_{0,N}^{(-)} &\longrightarrow \frac{(x-iy)^m}{(\tau - iz_0)^m} u_{0,N+m}^{(-)}, \end{aligned} \tag{46}$$

which conform to the rule that, if v is a solution of the wave equation, also $\frac{(x\pm iy)^m}{(\tau - iz_0)^m} v$ is a solution [8] (set $N-m$ in (46)), provided that

$$\left[\widehat{\mathcal{L}}_{\pm} - 2\frac{x+iy}{\tau - iz_0}\frac{\partial}{\partial \sigma}\right] v = 0,$$

the latter appearing as the 2D complexified version of (38).

As a final note, let us say that the transformations signified by (4) may be framed within the same scheme above discussed, resorting of course to symmetry operators that involve both space and time coordinates, i.e., replacing $\widehat{\mathcal{L}}_{\pm}$ by $\widehat{\mathcal{T}}_{\pm} = \frac{\partial}{\partial x} \pm i\frac{\partial}{\partial \mathfrak{y}}$ with $\mathfrak{y} = ict$.

6. LORENTZIAN-LIKE WAVE FUNCTIONS AND KLEIN-GORDON EQUATION

Strictly related to the question of the solutions to the wave equation has always been considered that of the solutions to the Klein-Gordon equation. Several approaches have been devised in this connection yielding both particular, i.e., valid under specific hypotheses and/or approximations, and general solutions of the latter [10, 11, 13, 24, 38–42]. Here, we simply deduce solutions to the Klein-Gordon equation which may be put in relation with the Lorentzian-like wave functions, illustrated in the previous sections.

As observed in [42], we may obtain possible solutions to the 3D Klein-Gordon equation

$$\left[\nabla^2 - c^{-2}\partial_t^2 - \left(\frac{mc}{\hbar}\right)^2\right] \mathfrak{u}(x, y, z, t) = 0, \tag{47}$$

through the 1D Fourier transform of those of a 4D homogeneous wave equation, just evaluated at $\Omega = \frac{mc}{\hbar}$. In symbols, we can write

$$\mathfrak{u}(x, y, z, t) = \int_{-\infty}^{+\infty} d\zeta e^{-i\Omega\zeta} u(x, y, \zeta, z, t)\Big|_{\Omega=\frac{mc}{\hbar}}, \tag{48}$$

where $u(x, y, z, \zeta, t)$ solves the 4D homogeneous scalar wave equation

$$\left[\nabla^2 + \partial_\zeta^2 - c^{-2}\partial_t^2\right] u(x, y, \zeta, z, t) = 0, \tag{49}$$

or, in terms of the characteristic variables $\tau = z - ct$ and $\sigma = z + ct$,

$$\left[\partial_x^2 + \partial_y^2 + \partial_\zeta^2 + 4\partial_\sigma\partial_\tau\right] u(x, y, \zeta, z, t) = 0. \tag{50}$$

In the sequel we will in general address the constant term entering the Klein-Gordon equation, which of course specifies in accord with the physical context of concern, as Ω^2 (in particular, $\Omega = \frac{mc}{\hbar}$ in (47), which in fact describes the dynamics of a relativistic massive particle with spin zero).

The usefulness of (48) stems evidently from the possibility of obtaining explicit forms of the Fourier integral for specific expressions

of $u(x, y, \zeta, z, t)$. In [42], for instance, it has been applied to suitable superpositions of Gaussian pulses in order to obtain what are there referred to as Gaussian packets for the Klein-Gordon equation in the case of both two and three space-variables.

Here we retain the axisymmetric Lorentzian-like form of the solutions to the wave equation, we dealt before, and hence we take

$$U_\delta(x, y, \zeta, z, t) = \frac{1}{(\tau - iz_0)^{\frac{3}{2}}} \left(\sigma + ia + \frac{x^2 + y^2 + \zeta^2}{\tau - iz_0} \right)^{-\delta} \tag{51}$$

which evidently solves (50) for any δ.

The above conforms to the general rule stated firstly in [21] and later re-derived in [10], concerning the relatively distortion-free solutions of the scalar wave equation of arbitrary (space) dimension $m > 1$. Accordingly, (51) is the 4D counterpart of s_δ in (6), which solves the 3D wave equation.

Then, on account of the integral (3.385.9) of [44], we can evaluate the Fourier integral in (48) in the specific case of (51) (see also (16)), thus obtaining the axisymmetric solution of (48) as

$$\mathfrak{u}_\delta(x, y, z, t) = (\tau - iz_0)^{\delta - \frac{3}{2}} \frac{1}{\beta^\delta(x, y, z, t)} W_{0, \frac{1}{2} - \delta}(2\Omega\beta), \tag{52}$$

where $W_{\kappa,\mu}$ denotes Whittaker's second function [30] and

$$\beta(x, y, z, t) = \sqrt{(\tau - iz_0)(\sigma + ia) + r^2}. \tag{53}$$

Note that $\beta = \sqrt{s_1}$, s_1 being given in (6).

According to the condition for the applicability of (3.385.9) of [44], expression (52), as derived from (48) with (51), should hold under the conditions that $\mathrm{Re}(\beta) > 0$ and $\delta > \frac{1}{2}$. Actually, a direct check assures that (52) solves (47) without any constraint on β and/or δ. In particular, (52) holds for $\delta = 0$ as well, which evidently yields the rather trivial solutions $\frac{1}{(\tau - iz_0)^{\frac{3}{2}}}$ and $\frac{1}{(\sigma + ia)^{\frac{3}{2}}}$ of (49), whose link to the splash-like wave functions is hardly recognizable.

We also note that interchanging τ and σ in (52) will provide alternative solutions of the Klein-Gordon equation, whose pulsed beam solutions follow from the known replacement $\sigma \to 2z$.

We recall here the symmetry properties of Whittaker's second function with respect to the change of sign of its indices, namely, [30]

$$W_{\kappa,\mu}(z) = W_{\kappa,-\mu}(z), \quad W_{-\kappa,\mu}(-z) = W_{-\kappa,-\mu}(-z),$$

as well as its relation to the modified Bessel function of second kind K_μ — already recalled in Section 2 — and consequently to the Hankel functions $H_\mu^{(1)}$, $H_\mu^{(2)}$:

$$W_{0,\mu}(z) = \sqrt{\frac{z}{\pi}} K_\mu\left(\tfrac{z}{2}\right) = \frac{i\sqrt{\pi z}}{2} e^{-i\mu\frac{\pi}{2}} H_\mu^{(1)}\left(\frac{iz}{2}\right),$$
$$W_{0,\mu}(iz) = \frac{\sqrt{\pi z}}{2} e^{-i\frac{\pi}{4}(1+2\mu)} H_\mu^{(2)}\left(\frac{z}{2}\right).$$

It may also be interesting to report the relation of $W_{0,\mu}(z)$ to the ordinary Laguerre polynomials $L_n^{(\alpha)}$ in correspondence of specific determinations of the second index μ [45], i.e.,

$$W_{0,\frac{1}{2}+n}(z) = (-)^n n! z^{-n} e^{-\frac{z}{2}} L_n^{(-2n-1)}(z),$$

which applies to our case when $\delta = j$, with j positive integer.

In particular, for $\delta = 0$ and $\delta = 1$ one obtains in (52) $W_{0,\frac{1}{2}}$ which simply implies an exponential function since $W_{0,\frac{1}{2}}(z) = e^{-\frac{z}{2}}$. Therefore,

$$\begin{aligned} \mathfrak{u}_0(x,y,z,t) &= \frac{1}{(\tau - iz_0)^{\frac{3}{2}}} e^{-\Omega\sqrt{(\tau-iz_0)(\sigma+ia)+r^2}}, \\ \mathfrak{u}_1(x,y,z,t) &= s_{\frac{1}{2}}(x,y,z,t) e^{-\Omega\sqrt{(\tau-iz_0)(\sigma+ia)+r^2}}, \end{aligned} \tag{54}$$

with $s_{\frac{1}{2}}$ being the splash pulse (6).

Figure 8 shows the 3D surface plots of the real and imaginary parts of $\mathfrak{u}_0$, $\mathfrak{u}_1$ and $\mathfrak{u}_{\frac{3}{2}}$ — apart from unessential multiplicative constants — vs. $\overline{r}$ and $\overline{z}$ at $\overline{ct} = 0$ and $\overline{ct} = 10$, the free parameters being set to $\overline{z}_0 = 10^{-1}$ and $\overline{a} = 20$. The oversigned symbols denote the respective quantity normalized to $\frac{1}{\Omega}$. Note that the vertical scales in the graphs have minor meaning since, in order to show both the real and imaginary parts in the same frame, the surface plots of the former have been shifted upward, the flat part of the relative surfaces actually corresponding to zero. We may see a certain localization of both the real and imaginary parts of the $\mathfrak{u}_\delta$'s at a minor extent when increasing δ.

Interestingly, an expression similar to that for $\mathfrak{u}_1(x,y,z,t)$ has been obtained in [40] (see Equation (11) there with $a_1 = a_3$) from a suitable weighted superposition over a free parameter of the focus wave mode solution of (47). In a sense, the expression (48) can be seen as a weighted superposition of what can be considered as solutions of

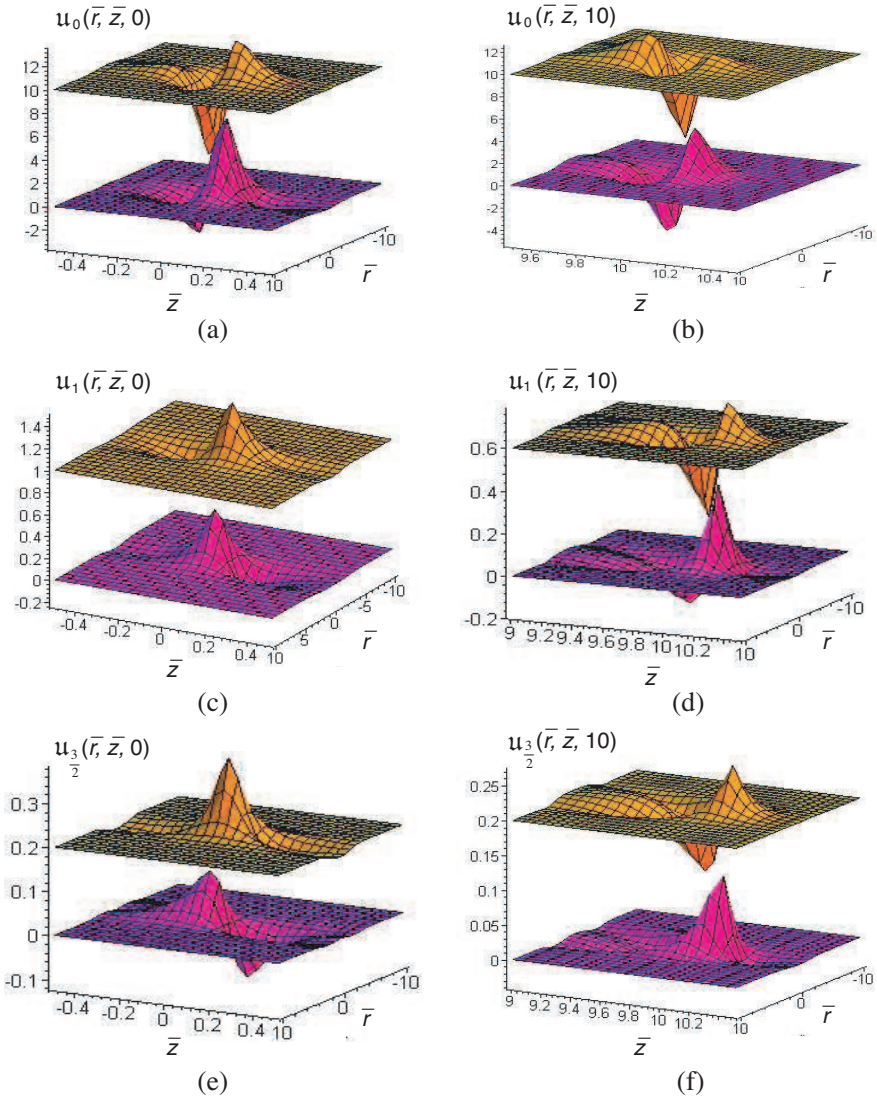

Figure 8. 3D plots of the real (upper surfaces) and imaginary parts (lower surfaces) of (a), (b) $\mathfrak{u}_0$, (c), (d) $\mathfrak{u}_1$ and (e), (f) $\mathfrak{u}_{\frac{3}{2}}$ vs. $\bar{r}$ and $\bar{z}$ at $\overline{ct} = 0$ and $\overline{ct} = 10$, the third argument of the $\mathfrak{u}$'s being here $\overline{ct}$. In all graphs, $\bar{z}_0 = 10^{-1}$ and $\bar{a} = 20$.

the 3D wave equation over the free parameter ζ, with the weighting function being just the simple harmonic $e^{-i\Omega\zeta}$.

It is evident that the solutions of the 2D scalar wave equation deduced in Section 3 in the form (25) can be used to obtain solutions of the 1D Klein-Gordon equation $[\partial_z^2 - c^{-2}\partial_t^2]\mathfrak{u}(z,t) = 0$. According to the properties of the Fourier integral, we see that the $\phi_{n,N}$'s, apart from unessential multiplying constants that involve powers of Ω, basically yield the same function, which in fact writes

$$\mathfrak{u}_N(z,t) = \frac{(\tau - iz_0)^{\frac{N-1}{2}}}{(\sigma + ia)^{\frac{N}{2}}} W_{0,\frac{1}{2}-N}\left(2\Omega\sqrt{(\tau - iz_0)(\sigma + ia)}\right). \qquad (55)$$

In Section 3, we limited ourselves to consider $N > 0$; this was functional to the possibility of introducing higher-order solutions related to the RHPs, whose definition implies $N > 0$. Of course, such a constraint here has no sense, so we can consider the case $N = 0$, which, as noted before, yields the trivial solutions $\frac{1}{\sqrt{\tau - iz_0}}$ and $\frac{1}{\sqrt{\sigma + ia}}$ of the 2D wave equation. In that case, one obtains $W_{0,\frac{1}{2}}$ in (55) just as with $N = 1$. In fact, the solutions corresponding to $N = 0$ and $N = 1$ differ only for the multiplying factor, involving $\tau - iz_0$ in the former case and $\sigma + ia$ in the latter case. Explicitly, we have

$$\begin{aligned} \mathfrak{u}_0(z,t) &= \frac{1}{\sqrt{\tau - iz_0}} e^{-\Omega\sqrt{(\tau - iz_0)(\sigma + ia)}}, \\ \mathfrak{u}_1(z,t) &= \frac{1}{\sqrt{\sigma + ia}} e^{-\Omega\sqrt{(\tau - iz_0)(\sigma + ia)}}, \end{aligned} \qquad (56)$$

in practice obtained one from the other by interchanging the terms $\tau - iz_0$ and $\sigma + ia$.

In Fig. 9, we show the $\overline{z}$-profiles of the real and imaginary parts of $\mathfrak{u}_0$ and $\mathfrak{u}_1$ as well as of the relative amplitudes at $\overline{ct} = 0$ and $\overline{ct} = 10$. As in the figures above, the coordinates as well as the various parameters are normalized to $\frac{1}{\Omega}$. As it can easily be inferred from the respective expressions, one basic difference between $\mathfrak{u}_0$ and $\mathfrak{u}_1$ is that the amplitude of $\mathfrak{u}_1$ decreases more quickly with $\overline{z}$ than that of $\mathfrak{u}_0$.

In conclusion, we may say that, in accord with the recipe (48), solutions of a m-dimensional Klein-Gordon equation generated by splash-like pulses write as ($x_m \equiv z$)

$$\begin{aligned} &\mathfrak{u}_\delta(x_1, \ldots, x_{m-1}, z, t) \\ = \; &(\tau - iz_0)^{\delta - \frac{m}{2}} \frac{1}{\beta^\delta(x_1, \ldots, x_{m-1}, z, t)} W_{0,\frac{1}{2}-\delta}(2\Omega\beta), \end{aligned} \qquad (57)$$

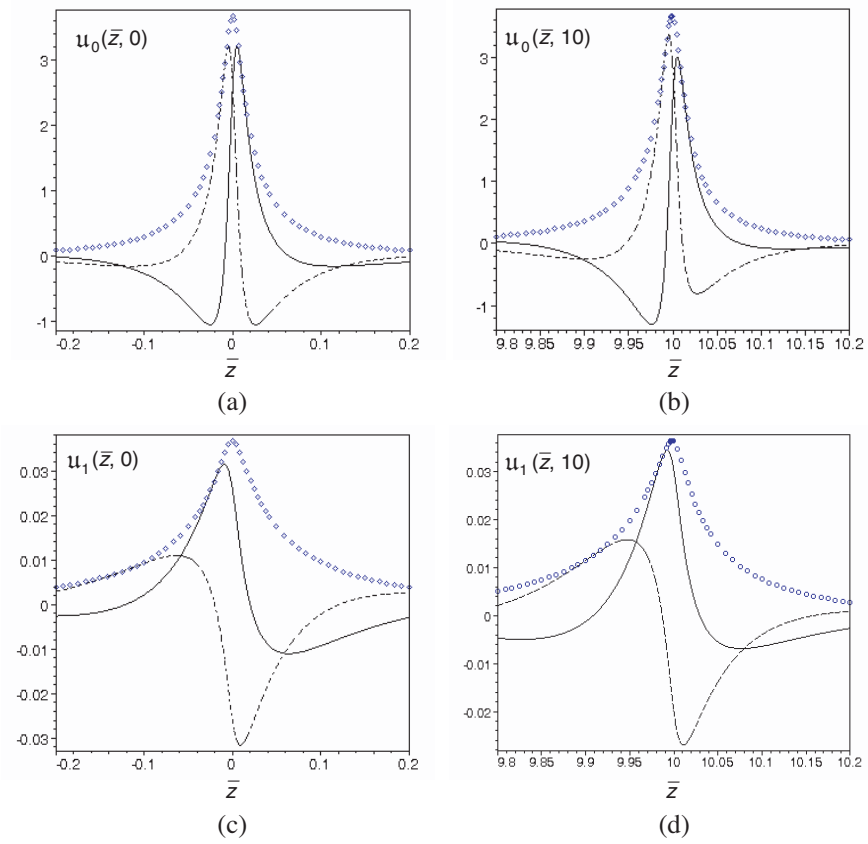

Figure 9. $\bar{z}$-profiles of the real parts (solid line), imaginary parts (dot-dashed line) and of the amplitudes (white diamonds) of (a), (b) $\mathfrak{u}_0$ and (c), (d) $\mathfrak{u}_1$ at $\overline{ct} = 0$ and $\overline{ct} = 10$, the third argument of the $\mathfrak{u}$'s being here $\overline{ct}$. In all graphs, $\bar{z}_0 = 10^{-2}$ and $\bar{a} = 10^2$.

with the m-dimensional version of β being evidently

$$\beta(x_1, \ldots, x_{m-1}, z, t) = \sqrt{(\tau - iz_0)(\sigma + ia) + \sum_{j=1}^{m-1} x_j^2}. \qquad (58)$$

More in general, let us say that non-axisymmetric forms for the splash pulses may be considered, like, for instance, in the case of $m+1$

space variables

$$U_\delta(x_1,\,\ldots,\,x_{m-1},\,\zeta,\,z,\,t)=\frac{1}{\sqrt{(\tau-iz_0)(\tau-iz_1)\ldots(\tau-iz_{m-1})}}$$
$$\left(\sigma+ia+\frac{x_1^2}{\tau-iz_1}+\ldots+\frac{x_{m-1}^2}{\tau-iz_{m-1}}+\frac{\zeta^2}{\tau-iz_0}\right)^{-\delta}, \tag{59}$$

which so yields the $(m+1)$-arbitrary constant dependent expression

$$\mathfrak{u}_\delta(x_1,\,\ldots,\,x_{m-1},\,z,\,t)$$
$$=\frac{(\tau-iz_0)^{\delta-\frac{1}{2}}}{\sqrt{(\tau-iz_1)\ldots(\tau-iz_{m-1})}}\frac{1}{\beta^\delta(x_1,\,\ldots,\,x_{m-1},\,z,\,t)}W_{0,\frac{1}{2}-\delta}(2\Omega\beta), \tag{60}$$

with

$$\beta(x_1,\,\cdots,\,x_{m-1},\,z,\,t)=\sqrt{(\tau-iz_0)\left[(\sigma+ia)+\sum_{j=1}^{m-1}\frac{x_j^2}{\tau-iz_j}\right]}, \tag{61}$$

as a possible solution to a m-dimensional Klein-Gordon equation.

We close the section noting that the expression for $\mathfrak{u}_1(z,t)$ in (56) has been obtained in [40] as well (see Equation (23) there setting $a_1 = a_3$), where it has been used to construct a solution to the 3D Klein-Gordon equation, i.e., $\mathfrak{u}_1(x,y,z,t)$ in (54), according to the method outlined in that reference. Evidently, inspecting the relations (60) and (61) we may recover within the present context the rule stated in [40], namely that one can pass from solutions of the 1D Klein-Gordon equation to solutions of the 3D equation, multiplying the expression (55) of the 1D solution by the factor $\frac{1}{\prod_{j=1}^{m-1}\sqrt{\tau-iz_j}}$ and replacing in it the characteristic variable $\sigma = z + ct \equiv \sigma_{1D}$ by

$$\sigma_{1D}=z+ct\rightarrow\sigma_{mD}=\sigma_{1D}+\sum_{j=1}^{m-1}\frac{x_j^2}{\tau-iz_j}.$$

It is easy to write down the alternative expressions in which the roles of the characteristic variables τ and σ are interchanged. Thus, for instance, with $m = 2$ (and $\sigma \leftrightarrow \tau$) in (60) and (61), one may recover the expression of the Gaussian packet for the 2D Klein-Gordon equation deduced in [42] (see Equation (14) there, with in particular the various parameters being set as $\nu = -\delta$, $\sigma = 0$ and $\varepsilon_1 = \varepsilon_2$.)

7. CONCLUSION

In [19] solutions of the free-space 3D scalar wave equation have been suggested, which resort to the splash pulses and have the RLPs as modulating factors of the basic splash-pulse waveform. A definite generation scheme for such solutions — referred to as Laguerre-Lorentzian solutions — have been deduced, which parallels that holding for the Laguerre-Gaussian pulses; both indeed are based on the same symmetry operators $\widehat{\mathcal{L}}_{\pm}$ of the wave equation.

Paralleling the analysis developed in [19], we have considered here solutions of the 2D scalar wave equation, which can be regarded as the 2D versions of the wave functions investigated in the aforementioned paper. In fact, these solutions involve the RHPs as modulating factors of what can be regarded as the 2D version of the basic splash-pulse waveform.

It has been recalled that the RHPs have been introduced as polynomial component of the quantum relativistic 1D harmonic oscillator wave function [25]. It has also been recalled that they have been recently re-considered within the context of the paraxial wave propagation in [26], where an "optical interpretation" of the *Hermite-Lorentzian* functions $\Phi_n^{(N)}$ has been suggested, enlightening their relation with the Lorentz beams, i.e., beams described by fields displaying a spatial dependence at the plane $z = 0$ of the type $\frac{1}{1+x^2}$. The latter have been introduced in [46] on the basis of the experimental observations reported in [47, 48].

Then, applying the rule (3), from the obtained 2D wave functions further solutions of the 3D wave equation — referred to as *Hermite-Lorentzian* solutions — have been constructed, which finally have been framed within the same generation scheme, that holds for the Laguerre-Lorentzian solutions, involving in fact the same operators $\widehat{\mathcal{L}}_{\pm}$ although through fractional, besides integer, powers.

As stressed in the Introduction, in our opinion, the unifying view — that emerges from the analysis here presented — of the 3D wave equation solutions of the splash-pulse type, deduced in the paper and in the previous quoted reference, is of interest at least from a mathematical viewpoint. As also stressed in the Introduction, in fact, we do not dwell here on the practical feasibility of the solutions that have been suggested, which evidently demand for further investigations.

In this regard, however, we simply recall that following the original hint, illustrated in detail in [24], an accurate analysis of the correspondence between source-free and aperture-generated MPS, splash and DEX pulses has been carried out in [16]. In particular, as

a result of such an analysis, the launchability of the splash pulses (at least for the values of the exponent δ considered in the paper) has been demonstrated to be possible with a maintenance of the features of the source-free field over a rather extended z-range between the near- and the far-field regions. The launching process, as described in [24], is based on the Huygens construction yielding the scalar field generated into $z > 0$ half-plane by the source aperture from the relevant initial excitation.

Accordingly, whereas the launchability of the $v_{0,N}$'s could be reasonably be assumed on account of the afore mentioned results in [16], we should face the issue concerning the launchability of the $u_{n,N}^{(\pm)}$'s.

It has also been recalled in the Introduction that in [18] the paraxial fields generated by $s_1(x, y, z, t) = \frac{1}{(\sigma+ia)(\tau-iz_0)+r^2}$ taken as a Hertz potential oriented transversely to the direction of propagation have been demonstrated to be the natural spatiotemporal modes of a cavity resonator, thus suggesting their production could be achieved by exciting a curved mirror resonator or the equivalent lens waveguide.

Finally, explicit expressions for the solutions of the Klein-Gordon equation, which in a sense can be considered as generated from the Lorentzian-like wave functions here discussed, have been deduced, also evidencing the relations with pertinent results already existing in the literature.

ACKNOWLEDGMENT

The author is pleased to acknowledge interesting discussions with Professor W. A. B. Evans, Dr. O. El Gawhary and Dr. S. Severini.

REFERENCES

1. Volterra, V., "Sur les vibrations des corps èlastiques isotropes," *Acta Math.*, Vol. 18, 161–232, 1894.
2. Bateman, H., "The conformal transformations of a space of four dimensions and their applications to geometrical optics," *Proc. London Math. Soc.*, Vol. 2, 70–89, 1909.
3. Bateman, H., "The transformations of the electrodynamical equations," *Proc. London Math. Soc.*, Vol. 8, 223–264, 1910.
4. Bateman, H., *The Mathematical Analysis of Electrical and Optical Wave-motion on the Basis of Maxwell's Equations*, Dover, New York, 1955.

5. Miller, W., *Symmetry and Separation of Variables*, Addison-Wesley, Reading, MA, 1977.
6. Hillion, P., "The Courant-Hilbert solution of the wave equation," *J. Math. Phys.*, Vol. 33, 2749–2753, 1992.
7. Hillion, P., "Generalized phases and nondispersive waves," *Acta Appl. Math.*, Vol. 30, 35–45, 1993.
8. Borisov, V. V. and A. B. Utkin, "Generalization of Brittingham's localized solutions to the wave equation," *Eur. Phys. J. B*, Vol. 21, 477–480, 2001.
9. Kiselev, A. P., "Generalization of Bateman-Hillion progressive wave and Bessel-Gauss pulse solutions of the wave equation via a separation of variables," *J. Phys. A: Math. Gen.*, Vol. 36, L345–L349, 2003.
10. Besieris, I. M., A. M. Shaarawi, and A. M. Attiya, "Bateman conformal transformations within the framework of the bidirectional spectral representation," *Progress In Electromagnetics Research*, PIER 48, 201–231, 2004.
11. Besieris, I. M., A. M. Shaarawi, and R. W. Ziolkowski, "A bidirectional traveling plane wave representation of exact solutions of the wave equation," *J. Math. Phys.*, Vol. 30, 1254–1269, 1989.
12. Kiselev, A. P., "Relatively undistorted waves. New examples," *J. Math. Sci.*, Vol. 117, 3945–3946, 2003.
13. Ziolkowski, R. W., "Exact solutions of the wave equation with complex source locations," *J. Math. Phys.*, Vol. 26, 861–863, 1985.
14. Hillion, P., "Splash wave modes in homogeneous Maxwell's equations," *Journal of Elecromagnetic Waves and Applications*, Vol. 2, 725–739, 1988.
15. Besieris, I. M., M. Abdel-Rahman, A. Shaarawi, and A. Chatzipetros, "Two fundamental representations of localized pulse solutions to the scalar wave equation," *Progress In Electromagnetics Research*, PIER 19, 1–48, 1998.
16. Shaarawi, A. M., M. A. Maged, I. M. Besieris, and E. Hashish, "Localized pulses exhibiting a missilelike slow decay," *JOSA*, Vol. 23, 2039–2052, 2006.
17. Hellwarth, R. W. and P. Nouchi, "Focused one-cycle electromagnetic pulses," *Phys. Rev. E*, Vol. 58, 889–895, 1996.
18. Feng, S., H. G. Winful, and R. W. Hellwarth, "Spatiotemporal evolution of focused singlecycle electromagnetic pulses," *Phys. Rev. E*, Vol. 59, 4630–4649, 1999.
19. Torre, A., "Relativistic Laguerre polynomials and the splash pulses," *Progress In Electromagnetics Research B*, Vol. 13, 329–

356, 2009.

20. Brittingham, J. N., "Packetlike solutions of the homogeneous-wave equation," *J. Appl. Phys.*, Vol. 54, 1179–1189, 1983.
21. Kiselev, A. P., "Modulated Gaussian beams," *Radiophys. Quantum Electron.*, Vol. 26, 755–761, 1983.
22. Belanger, P. A., "Packetlike solutions of the homogeneous-wave equation," *JOSA A*, Vol. 1, 723–724, 1984.
23. Sezginer, A., "A general formulation of focus wave modes," *J. Appl. Phys.*, Vol. 57, 678–683, 1985.
24. Ziolkowski, R. W., "Localized transmission of electromagnetic energy," *Phys. Rev. A*, Vol. 39, 2005–2033, 1989.
25. Aldaya, V., J. Bisquert, and J. Navarro-Salas, "The quantum relativistic harmonic oscillator: Generalized Hermite polynomials," *Phys. Lett. A*, Vol. 156, 381–385, 1991.
26. Torre, A., W. A. B. Evans, O. El Gawhary, and S. Severini, "Relativistic Hermite polynomials and Lorentz beams," *J. Opt. A: Pure Appl. Opt.*, Vol. 10, 115007, 2008.
27. Natalini, P., "The relativistic Laguerre polynomials," *Rend. Matematica, Ser. VII*, Vol. 16, 299–313, 1996.
28. Nagel, B., "The relativistic Hermite polynomial is a Gegenbauer polynomial," *J. Math. Phys.*, Vol. 35, 1549–1554, 1994.
29. Ismail, M. E. H., "Relativistic orthogonal polynomials are Jacobi polynomials," *J. Phys. A: Math. Gen.*, Vol. 29, 3199–3202, 1996.
30. Erdélyi, A., W. Magnus, F. Oberhettinger, and F. G. Tricomi, *Higher Transcendental Functions*, Vols. 1 and 2, MacGraw-Hill, New York, London and Toronto, 1953.
31. Heyman, E., "Pulsed beam propagation in inhomogeneous medium," *IEEE Trans. Antennas Prop.*, Vol. 42, 311–319, 1994.
32. Hillion, P., "A remark on the paraxial equation for scalar waves in homogeneous media," *Opt. Comm.*, Vol. 98, 217–219, 1993.
33. Hillion, P., "Paraxial Maxwell's equation," *Opt. Comm.*, Vol. 107, 327–330, 1994.
34. Wu, T. T., "Electromagnetic missiles," *J. Appl. Phys.*, Vol. 57, 2370–2373, 1985.
35. Shen, H.-M. and T. T. Wu, "The properties of the electromagnetic missile," *J. Appl. Phys.*, Vol. 66, 4025–4034, 1989.
36. Courant, R. and D. Hilbert, *Methods of Mathematical Physics*, Vol. 2, Interscience, New York, 1962.
37. Srivastava, H. M. and H. L. Manocha, *A Treatise on Generating Functions*, John Wiley and Sons, NY, 1984.

38. Shaarawi, A. M., I. M. Besieris, and R. W. Ziolkowski, "A novel approach to synthesis of nondispersive wave packet solutions to the Klein-Gordon and Dirac equations," *J. Math. Phys.*, Vol. 31, 2511–2519, 1990.
39. Donnelly, R. and R. Ziolkowski, "A method for constructing solutions of homogeneous partial differential equations: Localized waves," *Proc. R. Soc. London A*, Vol. 437, 673–692, 1992.
40. Besieris, I. M., A. M. Shaarawi, and M. P. Ligthart, "A note on dimension reduction and finite energy localized wave solutions to the Klein-Gordon and scalar wave equations. I. FWM-type," *Journal of Electromagnetic Waves and Applications*, Vol. 14, 593–610, 2000.
41. Besieris, I. M., A. M. Shaarawi, and M. P. Ligthart, "A note on dimension reduction and finite energy localized wave solutions to the Klein-Gordon and scalar wave equations. I. X wave-type," *Progress In Electromagnetics Research*, PIER 27, 357–365, 2000.
42. Perel, M. V. and I. V. Fialkovsky, "Exponentially localized solutions of the Klein-Gordon equation," *J. Math. Sci.*, Vol. 117, 3994–4000, 2003.
43. Kiselev, A. P. and M. V. Perel, "Relatively distortion-free waves for the m-dimensional wave equation," *Diff. Eq.*, Vol. 38, 1206–1207, 2002.
44. Gradshteyn, I. S. and I. M. Ryzhik, *Table of Integrals, Series and Products*, 7th Edition, Academic Press, New York, 2007.
45. Buccholz, H., *The Confluent Hypergeometric Function*, Springer-Verlag, Berlin, 1969.
46. El Gawhary, O. and S. Severini, "Lorentz beams and symmetry properties in paraxial optics," *J. Opt. A: Pure Appl. Opt.*, Vol. 8, 409–414, 2006.
47. Dumke, W. P., "The angular beam divergence in double-heterojunction lasers with very thin active regions," *IEEE J. Quantum Electron.*, Vol. 11, 400–402, 1975.
48. Naqwi, A. and F. Durst, "Focusing of diode laser beams: A simple mathematical model," *Appl. Opt.*, Vol. 29, 1780–1785, 1990.